Microwave conductivities of high-T_c oxide superconductors and related materials

2005 J. Phys.: Condens. Matter 17 R143

(http://iopscience.iop.org/0953-8984/17/4/R01)

INSTITUTE OF PHYSICS PUBLISHING JOURNAL OF PHYSICS: CONDENSED MATTER

J. Phys.: Condens. Matter **17** (2005) R143–R185 doi:10.1088/0953-8984/17/4/R01

TOPICAL REVIEW

Microwave conductivities of high-T_c oxide superconductors and related materials

A Maeda[1]**, H Kitano and R Inoue**

Department of Basic Science, The University of Tokyo, 3-8-1, Komaba, Meguro-ku, Tokyo 153-8902, Japan
and
CREST, Japan Science and Technology Cooperation (JST), 4-1-8, Honcho, Kawaguchi, Saitama 332-0012, Japan

E-mail: cmaeda@mail.ecc.u-tokyo.ac.jp

Received 3 December 2003, in final form 9 September 2004
Published 14 January 2005
Online at stacks.iop.org/JPhysCM/17/R143

Abstract
Recent studies of electromagnetic response at microwave- and millimetre-wave frequencies of the high-temperature cuprate superconductors and related materials are reviewed, with special interest in the experimental papers. These include the superfluid response in the superconducting state, quasi-particle responses below T_c, and characteristic charge excitations in related materials. We also discuss the electronic structure in the vortex core and superconducting fluctuation.

Contents

[1] Author to whom any correspondence should be addressed.

1. Introduction

The ac conductivity of materials includes a mine of important information on the electronic state and dynamics of electrons in those materials. Conductivity at optical frequencies reflects various kinds of elementary charge excitations. Experimental techniques and theoretical analyses have been well established for physics in the optical region [1, 2]. Recently, much interest has been taken in phenomena at lower frequencies of microwave- and millimetre-wave regions. A typical example is the collective charge excitation by quantum condensates, such as charge-density waves (CDWs) and spin-density waves (SDWs), exhibiting a large resonance in these frequency regions, together with a very large dielectric function [3]. Another example is the charge excitation in high-T_c cuprate superconductors. It is well established that in these materials the physical properties depend strongly on carrier doping [4]. In the phase diagram of temperature versus doping, various phases exist (or sometimes coexist), such as antiferromagnets, high-T_c superconductors, 'strange' metals, normal metals, etc. Even in the normal state of the 'strange' metals, a pseudogap opens at temperatures far above T_c for some range of doping, particularly for low doping. In the pseudogapped region, it is argued that various types of large fluctuations of charge and spin might contribute to physical properties. Thus, some of these fluctuations should show up in the ac conductivity at low energies. Recently, it has been suggested that the phase diagram of the cuprate superconductors can be interpreted from the more general point of view of quantum criticality [5]. This interpretation opens a possibility that new types of low-energy charge excitations are possible in strongly correlated materials as rather common phenomena. Therefore, it has become more and more important to investigate the ac conductivity in the microwave- to millimetre-wave frequency region.

In conventional superconductors, the microwave conductivity measurement (or the surface impedance measurement) has been one of the most popular tools to investigate properties of superconductors [6–8]. Since the discovery of high-temperature superconductivity in cuprates, the charge response at microwave- and millimetre-wave frequencies has been investigated more extensively in the superconducting state [9]. It gives detailed information on quasiparticle (QP) dynamics in the superconducting state. In particular, different from optical studies, this can provide detailed data of the charge response as a function of temperature. The reactive response gives information on the superfluid density. Detailed measurement of the temperature and magnetic-field dependence of the superfluid density gives information on the symmetry of the condensate wavefunction. Measurements at various frequencies at temperatures close to the superconducting transition temperature, T_c, provide information on the fluctuation of superconductivity. Since it is expected, in some theories, that the superconductivity fluctuation in cuprates changes largely as a function of hole concentration, it is interesting to discuss superconductivity fluctuation as a function of doping.

When magnetic field is applied to a superconductor, quantized magnetic vortices are formed, which respond to the alternating electromagnetic field. The complex impedance at microwave frequencies contains information on the pinning and viscosity of the vortex. In particular, the latter is closely related to the electronic structure of the quasiparticles (QPs) in the vortex core [10, 11].

In this article, we will give a brief review of the ac conductivity measurement in microwave- and millimetre-wave frequencies of cuprate based materials including the high-T_c superconductors, with special interest in the potential variety of this technique to explore the diverging aspects of charge excitation in solids, and will try to show how these techniques play important roles in understanding the physics of the above-mentioned issues.

The organization of the paper is as follows. In section 2, we will describe basic concepts important for understanding the contents of the following sections. In section 3, we discuss experimental techniques of the microwave conductivity measurement briefly. Because of the space limitation, we will mainly focus on the measurement techniques on bulk materials. There, we also focus on the underlying problems in the data analysis. In section 4, we will discuss the electromagnetic response of the high-T_c cuprate superconductors. Since an excellent review has already been written on this subject by Bonn and Hardy [9] in 1996, we will weight the results published after this article, and try to make this review complimentary to [9]. Section 5 will also be devoted to the topics related to the high-T_c superconductivity, but those in the presence of the magnetic field: the mixed state. In this section, we discuss the QP electronic structure in the vortex core, and will show how the microwave techniques play a crucial role for this subject. This is another issue that was not discussed in [9]. In section 6, we will focus on the research that tries to catch the dynamics of the collective charge excitations specific to the strongly correlated materials. There, we will discuss mainly studies concerning the dynamics of charge 'stripes', and ac conductivity of a spin ladder material. Finally, in section 7, we will summarize this topical review article.

Since the range of topics that microwave techniques covers is vast, it is impossible to give a complete and a self-contained review of all these subjects. Readers are strongly encouraged to read other reviews and related papers, cited at the relevant pages in this topical review article.

2. Complex conductivity and surface impedance of material

2.1. Complex conductivity

The complex electrical conductivity tensor at angular frequency ω, $\tilde{\sigma}(\omega)$, is defined as

$$\mathbf{j}(\omega) = \tilde{\sigma}(\omega)\mathbf{E}(\omega), \tag{1}$$

where $\mathbf{j}(\omega)$ and $\mathbf{E}(\omega)$ are the current density and the electric field at the same frequency, respectively. When $\mathbf{E}$ is small, usually $\tilde{\sigma}$ is independent of $\mathbf{E}$ (linear response). As will be discussed later, sometimes the nonlinearity becomes important.

In this article, we treat σ as diagonal, since we do not discuss the Hall effects or properties of materials with particularly low symmetry. Then, $\tilde{\sigma}$ is diagonal, and we will drop the tilde mark below unless there is a possibility of confusion. For materials such as high-T_c cuprates, the electrical properties are anisotropic. If necessary, we will use subscripts (or superscripts) such as σ_a, σ_b, and σ_c, representing the diagonal components in the corresponding crystallographic directions. We also use the expression σ_{ab}, representing the conductivity for the current in the CuO_2 plane (the ab plane).

The complex dielectric constant, $\epsilon(\omega)$, is related to the complex conductivity, $\sigma(\omega)$, as

$$\epsilon(\omega) \equiv \epsilon_1(\omega) - i\epsilon_2(\omega) \equiv (\sigma(\omega) - \sigma_{dc})/i\omega \equiv (\sigma_1(\omega) + i\sigma_2(\omega) - \sigma_{dc})/i\omega, \tag{2}$$

where dc conductivity, σ_{dc}, is subtracted for the definition of $\epsilon(\omega)$. The real and imaginary parts (denoted by the subscripts 1 and 2, respectively) of σ and ϵ are related to each other through the Kramers–Kronig relation.

In general, the current density and the electric field are dependent on space as well as time, as $\mathbf{j}(\mathbf{r}, t)$ and $\mathbf{E}(\mathbf{r}, t)$. As a result, $\mathbf{j}(\mathbf{r}, t)$ is expressed as a convolution as follows:

$$\mathbf{j}(\mathbf{r}, t) = \int_{-\infty}^{t} \int \sigma(\mathbf{r} - \mathbf{r}', t - t')\mathbf{E}(\mathbf{r}', t')\, \mathrm{d}\mathbf{r}'\, \mathrm{d}t'. \tag{3}$$

This is the *nonlocal* response because the conductivity and the electric field at the point $\mathbf{r}'$ near the point $\mathbf{r}$ can also contribute to the current density at the point $\mathbf{r}$. The Fourier transformation leads to the relation which is dependent on the wavenumber, $\mathbf{q}$, and the frequency, ω, as follows:

$$\mathbf{j}(\mathbf{q}, \omega) = \sigma(\mathbf{q}, \omega)\mathbf{E}(\mathbf{q}, \omega). \tag{4}$$

In nonmagnetic metals, the characteristic length scale of the spatial change of the electromagnetic field is the skin depth,

$$\delta \equiv \sqrt{\frac{2}{\mu_0 \sigma_1 \omega}}, \tag{5}$$

(μ_0 is the permeability of vacuum, σ_1 is the real part of the conductivity, and ω is the angular frequency). When δ is sufficiently larger than the mean free path, ℓ, of the electrons, the spatial change of the electromagnetic field around the point $\mathbf{r}$ is negligibly small. Thus, $\mathbf{E}$ in the integrand of equation (3) can be put outside the spatial integral, and the resultant relationship is

$$\mathbf{j}(\mathbf{r}, t) = \int_{-\infty}^{t} \sigma(\mathbf{r}, t - t')\mathbf{E}(\mathbf{r}, t')\, \mathrm{d}t'. \tag{6}$$

This is called the *local* response. For most metals including high-T_c cuprates, δ is larger than ℓ even at microwave frequencies, and the local response concept is valid. Only for ultra-pure metals with ℓ larger than δ does the nonlocality become important. Another important exception is the so-called type-I superconductor, which will be discussed later. Fourier transformation of equation (6) gives equation (1).

2.2. *Surface impedance: what do we measure?*

In extracting conductivity of a material, the most important parameter is the skin depth, δ. When δ is much smaller than the typical spatial dimension of the sample, L ($\delta \ll L$), what is measured directly is the complex surface impedance, Z_s, defined as

$$Z_s \equiv R_s - \mathrm{i}X_s \equiv \mathbf{E}_\parallel / \mathbf{H}_\parallel = \mathbf{E}_\parallel \Big/ \int_{-\infty}^{0} \mathbf{j}(z)\, \mathrm{d}z. \tag{7}$$

Here, R_s and X_s are the surface resistance and the surface reactance, respectively, $\mathbf{E}_\parallel$ and $\mathbf{H}_\parallel$ represent the components of the electric and magnetic fields parallel to the surface of the sample, and the integration of the current density $\mathbf{j}$ is made in the direction perpendicular to the surface. The coordinate z represents the distance from the surface in this direction. In the local limit, Z_s can be represented by the complex conductivity as

$$Z_s = \left[\frac{\mathrm{i}\mu_0 \omega}{\sigma_1 + \mathrm{i}\sigma_2}\right]^{1/2}. \tag{8}$$

Thus, by measuring the complex Z_s, we can deduce the complex σ, which should be compared to the theoretically calculated $\sigma(\omega)$ in various models.

In the opposite limit, where $\delta \gg L$, the electromagnetic field penetrates into the whole volume of the sample, and the complex conductivity (or the complex dielectric constant) can be obtained directly from the measured quantities. For intermediate cases between the above two extremes, there is no well established method for extracting conductivity from the measured quantities, even now. Therefore, measurements of materials whose conductivity (or dielectric function) changes by large orders of magnitude, such as the ones that undergo metal-to-insulator transition, is a rather challenging problem. Another difficult situation emerges when the real part of the dielectric function, ϵ_1, is very large. These will be discussed in section 3.2 briefly.

When one measures the microwave properties in the *ab* planes of the high-T_c cuprate single crystals, the situation that $\delta \ll L$ is almost always satisfied both in the normal and superconducting states. Therefore, the surface impedance measurements have mainly been performed. However, when one measures the *c*-axis properties perpendicular to the *ab* planes, careful considerations are required, since δ can be comparable to L, as will be discussed in section 4.4. Since the skin depth depends on frequency, this should always be recalled during the measurement. In particular, it has serious influences on the broadband measurement where the frequency is swept continuously, and also on the measurement of materials whose electrical conductivity is strongly temperature dependent.

In the next section, we describe various experimental techniques developed for the measurement of the surface impedance, Z_s, or the complex conductivity, σ, of the high-T_c superconductors and related materials. Problems in the data analysis process will also be discussed in detail.

3. Experimental aspects

3.1. Experimental techniques

Most of the high-T_c cuprate superconductors and related materials have very anisotropic electronic properties. Thus, single crystals or highly oriented, single-crystalline films are necessary to explore the physical properties[2]. In addition, high-quality single crystals are only obtainable with smaller dimensions than 1 mm. This makes the application of many measurement methods used for conventional superconductors to these new materials very difficult. In this subsection, we focus on the important developments of the measurement methods of Z_s using resonant or nonresonant techniques. Many of the important results discussed after this section would not be obtained without technical improvements reviewed in this section. In many cases, the cavity perturbation method using a resonator with high sensitivity has often still been used, since it is favourable for small single crystals, and it can measure Z_s (or σ) as a function of temperature and magnetic field precisely. The nonresonant broadband method can be used for obtaining σ as a function of the microwave frequency. This method is complementary to the resonant method, since the resonant method is performed at fixed frequencies. However, the microwave broadband method performed at low temperatures is technically challenging even now, which will be mentioned below.

3.1.1. Methods using resonators. In the cavity perturbation method [19–21], one measures the change of the resonance frequency f, Δf, and that of the quality factor Q, ΔQ, caused by

[2] Panagopoulos *et al* published many results on the penetration depth of high-T_c superconductors [16, 17] using magnetically aligned powders, based on the analysis [18] of ac magnetization data. A merit of this method is that it can determine the absolute magnitude of the penetration depth. In their analysis, however, they assumed the distribution of spherical small particles, which is unrealistic. Judging from the result, this method might be useful in discussing a crude tendency of the magnitude of the penetration depth as a function of carrier concentration, materials, etc.

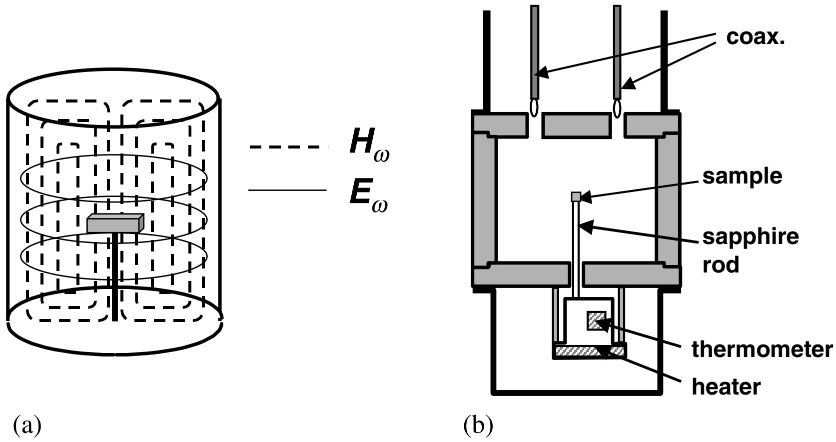

Figure 1. (a) The electromagnetic field of a TE_{011} cylindrical cavity resonator. (b) A cavity resonator in the 'hot-finger' method.

the insertion of the sample. The complex conductivity, σ $(=\sigma_1 + i\sigma_2)$, and surface impedance, Z_s $(=R_s - iX_s)$, can be obtained from these Δf and ΔQ. In the skin depth regime (SDR), where $\delta \ll L$, the surface resistance, R_s, and the surface reactance, X_s, are known to be proportional to ΔQ and Δf, respectively. In particular, for superconductors, $X_s = \mu_0\omega\lambda$, where λ is the so-called penetration depth. Thus, Δf measurement directly gives information on λ. It should be noted, however, that Δf measurement cannot give an absolute magnitude of λ. It gives only the change in λ, $\Delta\lambda$.

A circular cylindrical cavity resonator, which is made of oxygen free copper (OFC) and operated in TE_{011} mode, has often been used in the frequency range between 3 and 150 GHz [20]. Because of the small dimensions of the single crystal, the sample is typically inserted into the centre of the cavity resonator, which corresponds to the antinode of the microwave magnetic field ('enclosed perturbation'), as shown in figure 1(a).

An important development is the so-called 'hot-finger' technique, as shown in figure 1(b) [22, 23]. By using this technique, the sample is thermally isolated from the resonator, and is heated up to at least 200 K without changing the resonator temperature. This is particularly favourable for the measurements of high-T_c cuprates, where it is necessary to vary the temperature for a wide range, since the large temperature-dependent background of the cavity can be removed. Another important progress is the use of a superconducting resonator with very high sensitivity, where the inner wall of the cavity is coated by Pb (or Pb:Sn alloy), or the cavity is made of Nb [22, 23]. By maintaining it at an ambient temperature of 4.2 K, or by pumping the ^{4}He bath down to $\sim$1.5 K, Q values reach $\sim 10^6$–10^8, which can detect R_s of the order of a few $\mu\Omega$. In fact, many groups have used this superconducting resonator for the precise measurements of $Z_s(T)$ in the Meissner state of various high-T_c cuprates, as will be discussed in section 4. In the lower-frequency region ($\sim$0.3–3 GHz), a split-ring resonator [24, 25] or a loop-gap resonator [26] is effective, since the cylindrical cavity resonator at these frequencies is too large to be put on the cryostat. The small size and the excellent field homogeneity of this resonator are favourable for the increase of filling factor, whereas the stability of the resonator is limited. In particular, a superconducting loop-gap resonator with a special assembly that minimizes the motion of the sample has been developed by Hardy *et al* [26], in order to measure the magnetic penetration depth, λ $(=X_s/\mu_0\omega)$, precisely. A resonant LC circuit coupled with a tunnel diode (of an FET) operating at $\sim$10 MHz has also been used for the precise measurement of $\lambda(T)$ [27–31]. This LC circuit can also be operated under strong magnetic field, where the superconducting resonator cannot be operated.

In the cavity perturbation method, it is crucially important that reproducibility and stability are achieved between the measurements with and without the sample, since the net difference between the data in these two measurements reflects the intrinsic response of the sample. Typical sources giving rise to irreproducible and unstable operation have been discussed by Dressel *et al* [21]. For example, the use of any exchange gas to control the thermal link between the sample and the cryogen will have a serious influence on Δf, since even a slight change of the pressure of the exchange gas gives rise to a large frequency shift of the high-Q resonator. It is also effective to put the cavity resonator inside the vacuum can [32, 33], since a slight thermal expansion of the cavity immersed into the cryogen gives rise to Δf, sensitive to the level of the helium bath. With an OFC cavity [32] and the superconducting Nb cavity [33] put in the vacuum can, measurements down to 0.3–1 K were performed.

For high-T_c thin films, various types of resonators have often been used to measure R_s and λ, such as a parallel-plate resonator [34], a microstrip resonator [35], and a dielectric resonator [36], rather than the cylindrical cavity resonator. The application of these resonators to the measurements of λ have been reviewed briefly by Bonn and Hardy [9]. In many of these cases, the hot-finger technique cannot be available. Thus, it is necessary to calibrate the large temperature-dependent background of the thin-film resonator. To avoid this difficulty, the temperature dependence of λ of high-T_c thin films has been measured by using the two-coil mutual inductance method [37].

In the actual experiments, it is also important to develop a highly accurate and *real-time* method to determine Q and f of the resonator for the measured data points. Petersan and Anlage have compared several different methods and concluded that the nonlinear least-squares fit to the phase versus frequency is the most accurate and precise method when the S/N ratio is large, while the nonlinear least-squares fit to a Lorentzian curve is better for noisier data [38]. However, in general, the nonlinear least-squares fit requires iterated calculations and test processes for numerical convergence, which make the fitting algorithm very time consuming and more complicated. Recently, Inoue *et al* developed a new method, which contains only the *linear* least-squares fit to the complex transmission data [39]. This method, which is called the 'complex linear regression method', has a very high accuracy for the high-Q resonator with large S/N ratio.

3.1.2. Nonresonant methods. The nonresonant bolometric detection can resolve the microwave loss smaller than 0.1 nW. This method was originally used for superconducting Al to explore the superconducting gap frequency [7]. Moreover, for tiny crystals of the cuprate superconductors it was found to be very effective [40]. This technique has recently been applied to some studies investigating the frequency-dependent surface resistance (0.6–20 GHz) in the Meissner state [41, 42] (see section 4.3) and the Josephson plasma resonance in the Meissner and vortex states [44, 43] (see section 4.4). In particular, Turner *et al* [41, 42] have succeeded in improving the sensitivity of bolometric detection with a resolution of 1.5 pW at 1.3 K, corresponding to ΔR_s of $\sim 1\ \mu\Omega$ for a $1 \times 1\ \mathrm{mm}^2$ platelet crystal.

To obtain the complex response, on the other hand, the so-called broadband technique using a vector network analyser is indispensable. For cuprate superconductors, it has been developed by Booth *et al* [45]. In this technique, σ or Z_s is obtained from the complex reflection (or transmission) coefficients as a function of the microwave frequency (typically 45 to 20 GHz). This reflection technique has been applied to the study of the dynamical fluctuation conductivity near T_c [46] (see section 4.5). One of the technical difficulties in this method is the accurate calibration to remove the systematic errors of the transmission line system, since such errors are generally dependent on temperature. In one-port reflection geometry, the systematic imperfection of the measurement system is generally described by three error coefficients (12 parameters are required in two-port transmission geometry). At room temperature, they are determined at each frequency by using the three kinds of calibration standard which are commercially available. However, the calibration in a cryogenic system is much more difficult, since commercial calibration standards are no longer characterized at low temperatures, and the necessary use of long and lossy coaxial cable makes the transmission in the high-frequency region worse and nonreproducible. Booth *et al* performed calibration as follows. First they performed calibration only at room temperature, using the commercial standards. Next, they assumed that only one of the error coefficients was temperature dependent, and calibrated the system by measuring a short (or superconductor) at the lowest temperature. Tosoratti *et al* proposed a revised method for the calbration analysis [47]. However, even in this method, the calibration measurement was not performed at each temperature. Recently, Kitano *et al* [48] succeeded in performing calibration at any temperature down to $\sim$10 K in the frequency range from 45 MHz to 12 GHz, by applying a new calibration method proposed by Stutzman *et al* [49]. This method of calibration is better because there is almost no assumption on these error parameters, and all of these can be determined only by experiments at all temperatures.

The advantage of this broadband method is that the complex response can be obtained, while the disadvantage is a poor sensitivity compared to other bolometric or resonant techniques. Unfortunately, the sensitivity of the current vector network analyser is insufficient to detect the small loss of R_s in the superconducting state. Thus, for instance, for superconductors, measurements suitable for this techniques are limited to the ones close to T_c, or the ones in the mixed state. Further improvement should be achieved in a future study.

3.2. Problems in data analysis process

As was described in the previous section, the enclosed cavity perturbation method (including the hot-finger technique) has often been used for obtaining the complex conductivity, σ, of the high-T_c cuprates and the related materials. In this subsection, we focus on some problems in the data analysis process of this method. Many of them are also common to the analyses in other resonant or nonresonant techniques.

In the cavity perturbation method, the change due to the insertion of the small sample is often described by the reduced complex frequency shift, $\Delta\hat{\omega}/\omega_0$, defined as

$$\frac{\Delta\hat{\omega}}{\omega_0} \equiv \frac{\Delta f}{f_0} - \mathrm{i}\Delta\left(\frac{1}{2Q}\right), \tag{9}$$

where Δ represents the difference between the cavity resonator with the sample (the sample-loaded cavity) and the one without the sample (the empty cavity), and f_0 $(=\omega_0/2\pi)$ is the resonant frequency of the empty cavity. The data analysis in this method is an *inverse eigenvalue* problem of Maxwell's equations, and cannot be solved in general [19]. Thus, the procedure for obtaining σ depends largely on the relationship between the complex wavenumber $\hat{k}$ $(\equiv\omega_0\sqrt{\mu_0\epsilon})$ in the sample, the mean free path ℓ, and the dimension L of the sample.

Fortunately, in most of the high-T_c cuprate superconductors except for some materials discussed in section 6, the real part of $\hat{k}$ is negligibly small in the microwave region. In addition, the relation in the local electrodynamics can be applied to both the *in-plane* and *interplane* electrodynamics, since the mean free path ℓ is much smaller than δ (corresponding to the imaginary part of $1/\hat{k}$) in both cases. Thus, σ can be obtained straightforwardly from Z_s $(=R_s - \mathrm{i}X_s)$ data using equation (8).

In *the skin depth regime* (SDR), where $\delta \ll L$, $\Delta\hat{\omega}/\omega_0$ is simply described as follows:

$$\left[\frac{\Delta\hat{\omega}}{\omega_0}\right]_{\mathrm{SDR}} = C - \mathrm{i}GZ_{\mathrm{s}}, \tag{10}$$

where C and G are a metallic shift (the frequency shift caused by a perfect conductor) and a resonator constant, respectively, which are geometrically determined by the shape of the sample. For a general spheroid, C and G can be calculated [19]. However, it is almost impossible to estimate them easily for a platelet single crystal of high-T_{c} cuprates even by a numerical calculation, because of the highly anisotropic properties. Rather, they have been determined experimentally from the normal-state dc conductivity, σ_{dc}, of the same crystal, utilizing the Hagen–Rubens relation ($\sigma_2 \ll \sigma_1 \simeq \sigma_{\mathrm{dc}}$), which is valid for the low-frequency region ($\omega\tau \ll 1$; τ is the QP scattering time) in an ordinary Drude metal. In substituting this relation into equation (8), we obtain

$$R_{\mathrm{s}} = X_{\mathrm{s}} = \sqrt{\mu_0\omega_0/2\sigma_{\mathrm{dc}}}. \tag{11}$$

Thus, C is determined by equating $\Delta(1/2Q)$ to $C - \Delta f/f_0$, while G is determined by comparing the measured $\Delta(1/2Q)$ with the R_{s} calculated by equation (11) using σ_{dc} and ω_0. Indeed, this method has often been used for the analyses of the high-T_{c} cuprate superconductors [9] and some organic superconductors [21]. As was also emphasized by Bonn and Hardy [9], in the enclosed cavity perturbation, the most appropriate reference to determine C and G in the SDR should be a perfect conductor with the same dimensions as the sample. Unfortunately, such a perfect reference cannot be obtained in the actual experiments. Thus, it is necessary to consider the following two kinds of uncertainty. One is the difference between $1/Q$ of the empty cavity and that of the cavity with a perfect conductor inside. Since the perfect conductor does not dissipate energy at all, it will affect the electromagnetic field distribution in the resonator more strongly than expected within the framework of the perturbation. In principle, the influence of this uncertainty is dependent on the sample size, the measured frequency, and the coupling constant of the resonator. If the sample sizes are not too large, this uncertainty is negligibly small in the normal state. However, in the superconducting state, it can greatly affect the determination of R_{s} at the lowest temperature, as will be discussed in section 4.3. An effective method to check this is to measure another superconductor with much smaller λ and R_{s}. Bonn *et al* [50] have proposed the use of Pb:Sn alloy with the same dimensions as a high-T_{c} cuprate sample, and have estimated that this correction amounts to $\Delta(1/Q) \sim 10^{-9}$ at $\sim$4 GHz, which roughly corresponds to 7 $\mu\Omega$ in R_{s}. They have subtracted this correction from the measured data to obtain the intrinsic $R_{\mathrm{s}}(T)$ of the sample. Note that the loss for such a correction is comparable to R_{s} at the lowest temperature, suggesting that the correction of this uncertainty crucially affects the estimate of the residual surface resistance, R_{res}. The effect of R_{res} will be discussed in section 4.3 again.

The other uncertainty that should be considered is the effect of thermal expansion of the sample. Many groups have discussed this effect in extracting $X_{\mathrm{s}}(T)$ [21, 26, 51]. As was pointed out by Dressel *et al* [21], the thermal expansion of the sample causes the temperature-dependent metallic shift, $C(T)$. Since $X_{\mathrm{s}}(T)$ is given by $(C(T) - \Delta f(T)/f_0)/G$ in the SDR, this effect can lead to a large systematic error in the determination of $X_{\mathrm{s}}(T)$ (or $\lambda(T)$ for superconductors) with changing temperature. In addition, in the enclosed cavity (not hot-finger type), the thermal expansion of the cavity causes the temperature-dependent resonator constant $G(T)$. Tsuchiya *et al* have corrected these uncertainties by using linear thermal expansion coefficients of both the sample and the cavity [51]. On the other hand, Hardy *et al* have pointed out that the sample movement in the resonator made the reliable determination of $\lambda(T)$ difficult [26]. This motion is caused by the thermal expansion of a dielectric rod supporting the sample. In order to minimize this effect, they have developed a loop-gap resonator with a special assembly made of a thin-walled quartz tube. A brief description of this apparatus has also been given by Hosseini *et al* [52]. As will be discussed again in the next section, this resonator has played a crucial role in the determination of the temperature dependence of λ. However, the influence of the sample movement has not been investigated extensively by other groups using a cylindrical superconducting cavity resonator. In fact, it largely depends on the structure of the resonator, the size of the sapphire rod, and the configuration of the sample and the electromagnetic field. Lee *et al* have reported that the correction due to the thermal expansion of a sapphire rod with 0.5 mm diameter in a cylindrical Nb cavity was typically $\leqslant$10% of the total frequency shift (in particular, it was negligible below 30 K), while a sapphire disc resonator in a Nb shield was extremely sensitive to the sample movement [53]. Therefore, practically, it is preferable to estimate the influence of the sample movement by measuring the reference samples whose properties are well known.

When we measure Z_s as a function of magnetic field, the above-mentioned uncertainty is unimportant even in the superconducting state, since the data in zero field can be used as those of the nearly perfect reference. At a fixed temperature, the thermal expansion effect is also negligible.

In the opposite limit to the SDR, referred to as *the depolarization regime* (DPR), since $|\hat{k}L| \ll 1$, the electromagnetic field can be treated as approximately quasistatic (QS). Thus, the complex dielectric constant, ϵ ($=\epsilon_1 - \mathrm{i}\epsilon_2$), can be obtained from $\Delta\hat{\omega}/\omega_0$ for the antinode of the microwave electric field. The following Buravov–Shchegolev formula has been used widely [54].

$$\left[\frac{\Delta\hat{\omega}}{\omega_0}\right]_{\mathrm{DPR}} = -\frac{\gamma}{N}\frac{\epsilon - 1}{\epsilon - 1 + (1/N)}. \tag{12}$$

Here, γ is a geometrical constant determined by the resonance mode and the ratio of the sample volume to the cavity volume [19], and N is the depolarization factor in the direction of applied microwave electric field. Although, strictly speaking, N cannot be defined for nonellipsoidal samples, the so-called ellipsoidal approximation is effective for such samples. In the DPR, the factors of γ/N and γ/N^2 play a similar role to the metallic shift, C, and the resonator constant, G, in the SDR, respectively. For the high-T_c cuprates and the related materials, equation (12) has been used for analysing the interlayer electrodynamics of $Bi_2Sr_2CaCu_2O_y$ (BSCCO) and the charge dynamics in the quasi-one-dimensional spin ladder compounds (see sections 4.4 and 6, respectively). In the actual analyses, we can experimentally determine the factor γ/N by utilizing the fact that $\Delta(1/2Q)$ shows a peak when external parameters such as temperature and magnetic field change (the so-called depolarization peak in dielectrics and the Josephson plasma resonance for layered superconductors), while the factor γ/N^2 is determined such that the resultant ϵ_1 (or σ_1) is consistent with dc and optical data.

It should be noted that the data analysis by the Buravov–Shchegolev formula is not always valid for poorly conductive materials. In particular, for highly dielectric materials with a very large dielectric constant such as the CDW state, the real part of $\hat{k}$ is no longer negligible. Thus, the above assumption for the DPR ($|\hat{k}L| \ll 1$) collapses. In such a highly dielectric region (HDR), $\Delta\hat{\omega}/\omega_0$ shows pseudo-periodic behaviour as a function of ϵ_1, which makes the extraction of ϵ from $\Delta\hat{\omega}/\omega_0$ difficult [55].

When we investigate the various phases in the carrier concentration versus temperature phase diagram of high-T_c cuprates and the related materials, we often encounter the situation in which experimental data exist in the crossover region between the SDR and the DPR. It is not easy to extract σ in such an intermediate region, since it is not straightforward to connect between SDR and DPR continuously. Evidently, the QS approximation (valid for the DPR), where the field inside the sample is assumed to be uniform, is broken down in the SDR.

As an approach to connect between the DPR and the SDR, an extended quasi-static (EQS) approximation has been tried. In this method, the field inside the sample is described by the Helmholtz equation, $(\nabla^2 + k^2)\mathbf{E}$ (or $\mathbf{H}$) $= 0$. For an isotropic spherical sample, several approximating solutions have been obtained under this EQS approximation [56–58]. Recently, Inoue *et al* have investigated the limit of applicability of such approximating solutions in the crossover region from DPR to SDR, by using a double-sphere model, in which the full Maxwell equations can be solved analytically [59, 60]. They also derived a new approximating formula for the spherical sample from the exact solutions, which were the extended version of the Champlin–Krongard formulae [56] and can be applied throughout the crossover region. From the experimental point of view, Ong has proposed the graphical method based on the Buravov–Shchegolev formula in the QS approximation, as an aid to obtain σ from the experimental data [61]. Kitano has applied this method to a high-T_c cuprate, BSCCO, based on the Champlin–Krongard formulae in the EQS approximation [62]. To sum up, the data analysis in the crossover region between the SDR and the DPR has not been well established yet. Further study, using a large-scale electromagnetic field simulator etc, might be important.

4. Superconductivity of high-T_c cuprate superconductors

4.1. Electromagnetic response of superconductors

The electromagnetic response of a superconductor in weak fields provides one of the most essential features of superconductivity, because in the dc limit it corresponds to the Meissner–Ochsenfeld effect,

$$\mathbf{j} = -\frac{1}{\mu_0 \lambda_L^2}\mathbf{A}, \tag{13}$$

where

$$\lambda_L^{-2} = \frac{\mu_0 n e^2}{m^*}. \tag{14}$$

Here, μ_0 is the permeability of vacuum, $\mathbf{j}$ is the current density, $\mathbf{A}$ is the vector potential, which is related to the magnetic field, $\mathbf{B}$, as rot $\mathbf{A} = \mathbf{B}$, e is the electronic charge, and n and m^* are the number density and the effective mass of electrons, respectively. Combining equation (13) with the Maxwell equation, it was found that the electromagnetic field inside the superconductor decays as $A \sim A_0 e^{-x/\lambda_L}$, where x is the distance from the surface of the superconductor. Thus, λ_L is found to be an important length scale of the spatial change of electromagnetic field in the superconductor (London penetration depth) [12]. For $T \simeq 0$ K, there is almost no quasiparticle (QP) that can dissipate energy, and equation (13) is valid even at finite frequencies, provided that $\hbar\omega \ll \Delta$ (Δ is the energy gap of the superconductor). Then, the conductivity at the frequency ω can be expressed as

$$\sigma(\omega) \simeq \left(\frac{1}{\mu_0 \lambda_L^2}\right)\left[\frac{1}{\mathrm{i}\omega} + \delta(\omega)\right] \tag{15}$$

since the electric field $\mathbf{E}$ is given by $\mathbf{E} = -\frac{\partial}{\partial t}\mathbf{A}$, and the δ function at $\omega = 0$ is related to the imaginary part by the Kramers–Krönig relation. Equation (15) means that (1) the Meissner–Ochsenfeld effect is equivalent to the infinite conductivity in the dc limit and (2) for $T \simeq 0$ K or for low frequencies σ is almost pure imaginary with a very small σ_1.

At finite temperatures, QPs are excited thermally above the superconducting energy gap. This causes the change in n_s, leading to the temperature-dependent λ_L. With increasing

Table 1. $D(E)$ and the exponent of $\Delta\lambda_L(T)$ versus node geometry of the superconducting order parameter.

Node geometry	$D(E)$	Exponent n ($\lambda \propto T^n$)
Fully gapped	0	Thermally activated
Points	E^2	2
Lines	E	1
Gapless	Constant	2

temperature, QPs are excited more and more. Thus, λ becomes longer. According to the BCS theory [13], λ_L at a temperature T, $\lambda_L(T)$, of a clean superconductor is given as [15]

$$\lambda_L^{-2}(T) = \lambda_L^{-2}(0)\left[1 - 2\int_\Delta^\infty \left(-\frac{\partial f}{\partial E}\right) D(E)\,\mathrm{d}E\right], \tag{16}$$

where f is the Fermi distribution function of the QP with energy E, and $D(E)$ is the density of states (DOS) of the QPs.[3] In particular, at low temperatures, where the gap magnitude is almost temperature independent, the change of $\lambda_L(T)$, $\Delta\lambda_L(T)$, is thermally activated,

$$\lambda_L(T)^{-2} \simeq \lambda_L(0)^{-2}\left[1 - \sqrt{\frac{2\pi\Delta}{k_\mathrm{B}T}}\exp\left(-\frac{\Delta}{k_\mathrm{B}T}\right)\right]. \tag{17}$$

These are characteristic of the phonon-mediated pairing in the BCS theory, where the Cooper pair wavefunction is s-wave-like, and the gap in the QP excitation spectrum is fully opened on the Fermi surface. However, in many superconductors these are of current interest; the Cooper pair wavefunction is considered to be anisotropic. This is because various kinds of correlation effect between electrons favour the pairing with finite angular momentum. Such anisotropic Cooper pairs are well known in the superfluidity of liquid ^{3}He. The symmetry of the pair wavefunction is determined by the kind of interaction and the symmetry of the crystal [63]. For such anisotropic Cooper pairs, the gap parameter, Δ, also depends on the momentum, $\mathbf{k}$, and it will vanish for special directions in the $\mathbf{k}$ space. In this case, QP excitation is possible even very close to the Fermi energy, and the QP DOS behaves typically as

$$D(E) \propto E^n, \tag{18}$$

where the exponent n is determined by the topology of nodes in the gap [63]. For lines of nodes $n = 1$, whereas for points of nodes $n = 2$. This leads to the $\Delta\lambda_L(T)$ with a power law form,

$$\Delta\lambda_L \propto T^k, \tag{19}$$

and the exponent k also reflects the topology of the nodes. These are summarized in table 1. Therefore, in principle, the low-temperature penetration depth measurement can probe the pairing mechanism of superconductivity.

When QPs exist in the superconductor, they dissipate energy and cause a finite σ_1. The general form of the conductivity was calculated by Mattis and Bardeen [64]. The qualitative behaviour is shown in figure 2. Since, at low temperatures, quasiparticles are created by the thermal excitation above the energy gap, the temperature dependence of conductivity, $\sigma(T)$, shows a thermally activated behaviour for an s-wave (isotropic) superconductor. Lack of QP in the low-temperature limit also leads to vanishingly small R_s as

$$R_\mathrm{s}(T) \propto \frac{(\hbar\omega)^2}{k_\mathrm{B}T}\ln\left(\frac{4k_\mathrm{B}T}{\hbar\omega}\right)\exp\left(-\frac{\Delta}{k_\mathrm{B}T}\right). \tag{20}$$

[3] For superconductors including QPs with finite mean free path, ℓ, the temperature dependence of the penetration depth, λ ($\lambda(T)$), changes slightly from $\lambda_L(T)$.

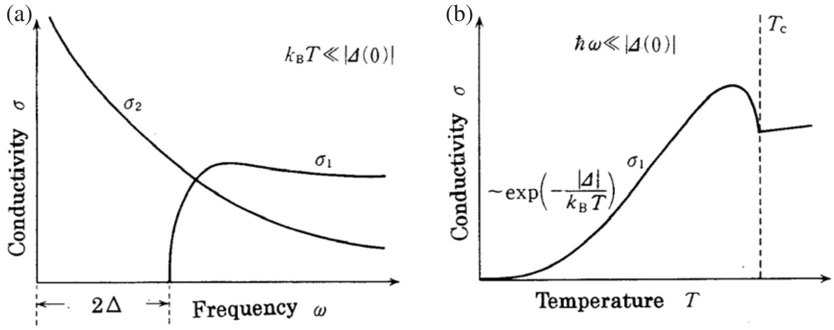

Figure 2. Conductivity of superconductor. (a) Frequency dependence at low temperature. The δ function at $\omega = 0$ is omitted. (b) Temperature dependence at a low frequency.

In contrast, for anisotropic superconductors with nodes in the gap, σ_1 also shows a power-law behaviour because of the same physics for $\lambda(T)$. For instance, for a $d_{x^2-y^2}$ wave superconductor, it is expected that $\sigma(T) \propto T^2$, very generally [65].

On the other hand, close to T_c, σ_1 shows a very prominent feature. That is, $\sigma_1(T)$ of the s-wave (BCS) superconductor [13, 14] exhibits a large enhancement below T_c (the so-called coherence enhancement) (figure 2(b)). The coherence enhancement was first observed in the NMR experiment [66], but it was rather recently even in conventional superconductors that the same effect was observed in the ac conductivity measurement [67]. Since this enhancement is due to the diverging DOS at the Fermi energy E_F, (1) this effect is more prominent for lower frequencies, and (2) this effect is strongly suppressed for the gap with nodes. These will be discussed in section 4.2, again.

To be more quantitative, there is no universal dependence of σ as a function of temperature, frequency etc, because it depends on the mean free path of the QP, ℓ. Another complexity is introduced because in superconductors a finite size is necessary for a wavepacket to be formed by the superconducting charge carriers. The smallest size is called the coherence length, ξ [6], which is another very important length scale characteristic of superconductors, and is given as

$$\frac{1}{\xi} = \frac{1}{\xi_0} + \frac{1}{\ell}, \tag{21}$$

where ξ_0 is the Pippard coherence length, which was given by the uncertainty relations as

$$\xi_0 = \frac{\hbar v_F}{\pi \Delta_0} \tag{22}$$

(Δ_0 is the energy gap at $T = 0$ K). Because of the finite coherence length, the electromagnetic response of superconductors is nonlocal, in general. The nonlocal formula was calculated by the BCS theory [64, 68, 69], and is given in textbooks (see for example [15]). Nonlocality is only important in superconductors with $\xi > \lambda$, which are mostly the so-called type-I superconductors. Fortunately, for high-T_c superconductors, $\lambda \gg \xi$ is valid in most cases. Thus, by a similar discussion as in section 2.1, the electromagnetic response can be regarded as local (the local limit (London limit)), and the nonlocal equation reduces to equation (13).

Experimentally, in most of the measurements of superconductors, we measure the surface impedance Z_s, since the penetration depth λ is much smaller than the sample dimension, L.

4.2. Symmetry of condensate wavefunction

4.2.1. Temperature dependence of penetration depth. For high-T_c cuprates, many works have been published on penetration depth, λ, measured by the electromagnetic response, since the symmetry of the condensate wavefunction is very important information for understanding the mechanism of high-T_c superconductivity. However, it is also well known that $\Delta\lambda(T)$ is very sensitive to the morphology and defects of the samples, particularly for high-T_c cuprates. Therefore, we will restrict our attention to studies performed for bulk 'single' crystals or very high-quality 'single-crystalline' films.

Since cuprate superconductors are quasi-two-dimensional, we should distinguish λ for shielding current flowing in the CuO_2 plane and that for perpendicular to the CuO_2 plane. Usual nomenclatures are λ_{ab} for the former, and λ_c for the latter. For a while, we will focus on λ_{ab}, and will not write the subscript 'ab'. The anisotropy of λ will be discussed in section 4.4.

At a very early stage, few studies discussed the low-temperature behaviour of $\lambda(T)$ [70]. All of the subsequent studies reported a T^2 behaviour [30, 71–73]. A breakthrough was brought by Hardy *et al* [26], who reported a clear T-linear dependence of λ as a function of temperature in a high-quality, optimally doped $YBa_2Cu_3O_y$ (YBCO) crystal[4]. As has already been mentioned, they paid a great deal of attention to preventing even very slight displacement of the crystal during the measurement, so that they used a loop-gap resonator, where the electromagnetic distribution inside the resonator is very uniform[5]. Thus, their data made a large number of the high-T_c community think it is convincing. Subsequent studies succeeded in reproducing the T-linear behaviour in YBCO [78], BSCCO [53, 79–81], and $Tl_2Ba_2CuO_6$ [82], probably because of the improvements in crystal qualities.

The T-linear behaviour suggests the presence of line nodes in the order parameter. Theoretically, it had been pointed out that the spin-fluctuation mechanism of the pairing on the CuO_2 plane favours the $d_{x^2-y^2}$ pairing, which has lines of nodes [83]. For this case, since $N(E)/N_0 = E/\Delta_0$ (Δ_0 is the maximum gap, and $N(E)$ and N_0 are the QP DOS in the superconducting state with the energy E and that at the Fermi level in the normal state, respectively),

$$\frac{\Delta\lambda}{\lambda(0)} \simeq (\ln 2)\frac{T}{\Delta_0}. \tag{23}$$

The data in [26] also showed a good agreement in the coefficient of the temperature derivative. However, $\lambda(T)$ data only provide the information on the topology of nodes (lines, points etc). More strictly speaking, $\lambda(T)$ data do not provide any information on whether there is a finite gap opened with the magnitude smaller than the lowest temperature measured. Now, together with the angle-resolved photoemission spectroscopy (ARPES) data [84] and those in phase sensitive interference experiments [85], it is well established that these penetration depths provided a strong support for unconventional ($d_{x^2-y^2}$-wave) pairing for almost optimally hole-doped high-T_c cuprate superconductors.

[4] Recently, it was established that the use of $BaZrO_3$ (BZO) crucibles resulted in YBCO crystals with at least one order of magnitude increase in purity (~99.995%), compared with that of YSZ (yttria-stabilized zirconia) crucibles [74]. However, considerable care should be taken for oxygen annealing for such extremely high-quality crystals. Srikanth *et al* measured Z_s of such high-purity crystals, and reported an anomaly in $\lambda(T)$ below T_c, suggesting the presence of another superconducting transition [75]. However, Kamal *et al* have confirmed that there was no evidence for two order parameter components in both $\lambda(T)$ and $R_s(T)$, using a similar ultra-purity BZO-grown crystal [76, 77]. They discussed that the oxygen vacancies in the higher-purity BZO-grown crystals had a tendency to cluster, acting as electronic scattering centres similar to intentionally doped impurities.

[5] In addition, they used the $H \parallel ab$ configuration because in this configuration the demagnetizing effect is less prominent for typical crystal pieces of YBCO.

$La_{2-x}Sr_xCuO_4$ (LSCO) is an exception, where the T-linear behaviour has never been reported both in bulk crystals [86] and in thin films [87]. This is probably due to the difficulty in preparing good crystals or films of this material. The authors in [87] argued that the result was consistent with the unconventional pairing, because the T^2 behaviour corresponding to the gapless state can only be realized for heavily damaged samples with a large number of magnetic impurities for conventional pairing. In magnetically aligned powder samples, the T-linear behaviour was reported by the measurements of static magnetic susceptibility [17]. However, as was mentioned in section 3, $\lambda(T)$ data in this method were extracted based on many assumptions, and the information on the temperature dependence is less reliable. The final conclusion should wait until measurements in single crystals or single-crystalline films with superior quality are performed.

To investigate the mechanism of superconductivity in terms of the $\lambda(T)$ study, important tests in the next stage are to explore (1) the dependence on disorder, (2) the dependence on carrier concentration, and (3) $\lambda(T)$ in electron-doped cuprate superconductors.

The effect of disorder was investigated in YBCO by Bonn *et al* [50]. As has already been summarized by Bonn and Hardy [9], only a small amount ($\sim$0.15%) of nonmagnetic Zn impurities, which substitute for Cu, caused a change from T-linear to T^2 behaviour in $\lambda(T)$ without appreciable reduction in T_c. On the other hand, a larger amount (0.75%) of magnetic Ni impurities was found not to alter the T-linear behaviour. These results were quite contrary to what was expected in the conventional BCS theory, where disorders with magnetic moments destroy superconductivity more strongly than nonmagnetic disorders. In a d-wave scenario, this surprising behaviour has been interpreted to mean that Zn impurities played the role of resonant (unitary) scatterer, which leads to a large pair-breaking effect, while Ni impurities behaved as a Born scatterer [88]. Recently, a local STM experiment was performed by Pan *et al* [89], which clarified the different roles between Zn and Ni impurities. The former created a sharp resonant peak in the QP DOS at the Fermi level, E_F, whereas the latter created a similar peak at a finite energy far from E_F. This difference has been explained theoretically [90].

Investigation of the dependence of $\lambda(T)$ as a function of carrier concentration, x, is not easy, since changing carrier concentration often affects the quality of the single crystals considerably. Here, we focus only on the reports for YBCO crystals. Bonn *et al* [91] investigated the dependence on doping of $\lambda(T)$ from the underdoped to the slightly overdoped crystals, and found that the T-linear behaviour was independent of x, strongly suggesting that the condensate wavefunction is $d_{x^2-y^2}$-like for almost all the ranges of hole doping. More surprisingly, the plots of $\lambda^2(0)/\lambda^2(T)$ versus T/T_c showed a remarkable universality over the entire temperature range. Since $1/\lambda^2(0)$ is roughly proportional to x in the underdoped region ('Uemura' plot) [92], it is suggested that the superfluid density, ρ_s ($\propto 1/\lambda^2$) for various x values, was described as $\rho_s(x, T) \approx ax - bT$ (a and b are numerical constants) at low temperatures. Lee and Wen [93] pointed out that neither the usual BCS model with d-wave symmetry nor the t–J model with $U(1)$ gauge formulation will ever be able to explain this behaviour as x goes to zero. This paradoxical relation has been mysterious for the last decade. Very recently, Hosseini *et al* [94] succeeded in investigating the doping and temperature dependence of ρ_s along the c axis close to the superconductor–nonsuperconductor boundary. Motivated by this result, Sheehy and co-workers [95] have proposed a unified theory of the doping and temperature dependence of ρ_s both in the ab planes and in the c direction. We will discuss this again in section 4.4.

Symmetry of the electron-doped cuprate is an important touchstone for investigating the mechanism of superconductivity in cuprate, since a resonating-valence-bond-based picture expects a symmetry of the physical properties between hole-doped and electron-doped cuprates [96], whereas other mechanisms do not necessarily expect such a symmetry.

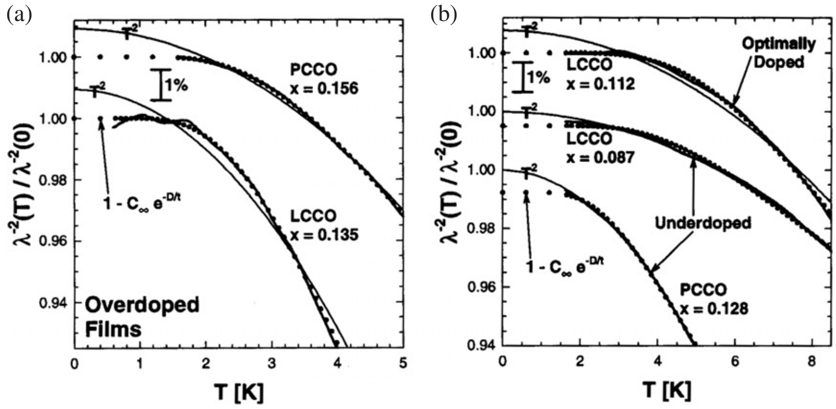

Figure 3. Temperature dependence of λ of PCCO and $La_{2-x}Ce_xCuO_4$ (LCCO): (a) overdoped, (b) optimally doped and underdoped [108].

Conclusions obtained by experimental studies have been diverging. Since tunnelling studies [97–99] proposed a fully gapped order parameters, whereas a SQUID experiment [100] and an ARPES experiment [101] proposed a d-wave order parameter. Even restricting our interest to the electromagnetic response, electron-doped cuprates have had a complex history. Wu *et al* [102] reported the thermally activated behaviour of $\lambda(T)$ for $Nd_{2-x}Ce_xCuO_4$ (NCCO). However, Cooper [103] pointed out that this was due to the temperature dependence of the magnetic moment of Nd (note that for magnetic materials $X_s = \mu\omega\lambda$, where μ is the permeability of the material). Another problem in electron-doped cuprate is the difficulty in preparing good crystals. Recently, however, good films have become available from an NTT group [104]. A study in a good $Pr_{2-x}Ce_xCuO_4$ (PCCO) film, which does not have magnetic moment, revealed a thermally activated behaviour [105], whereas Prozorov *et al* [106] and Kokales *et al* [107] reported T^2 (or T^α) behaviour in PCCO crystals and films from different laboratories. Recently, Skinta *et al* [108] investigated the dependence of $\lambda(T)$ on carrier doping for films from the NTT group [104]. They found that the overdoped and the optimally doped samples exhibited thermally activated behaviour, whereas the underdoped sample showed the T^2 behaviour (figure 3). Thus, they suggested the presence of a phase transition from d-wave to s-wave state as a function of doping. A similar crossover (or transition) was also proposed by a point contact spectroscopy study [109]. A more recent study by the same group down to lower temperatures using improved films with a buffer layer between the film and the substrate proposed a full gap opening ($\Delta/k_B T_c = 0.3$–1.0, smaller than the BCS value of 1.74) for all samples in a wide range of doping [110]. Another recent study on PCCO films [111] reported that all the films showed T^2 behaviour down to 0.35 K. However, the dc resistivity values of their films are higher by an order of magnitude than the ones in [110], especially for underdoped films.

After all, no consensus has been formed on the temperature dependence of λ_{ab} in electron-doped cuprates, even now. Probably, the origin of the controversy is the difficulties in controlling the sample characteristics of electron-doped cuprate superconductors. A comparative, comprehensive study by different experimental methods using well characterized crystals (or films) from the same laboratory is the only way to resolve the controversy.

In summary, for hole-doped cuprate superconductors, except for LSCO, a clear T-linear behaviour of λ has established the d-wave nature of the condensate. Quantitative understanding of the doping dependence of $d\lambda(T)/dT$ had been a long puzzle. Recently, theoretical understanding just started.

On the other hand, the symmetry of the condensate wavefunction of electron-doped cuprate superconductors has still been in controversy. Since the study of pairing symmetry plays an essential role to restrict the possible theories on the mechanism of superconductivity, further improvements of sample preparation and characterization are earnestly desired.

4.2.2. Magnetic field dependence of penetration depth. Penetration depth depends on magnetic field, H, even very slightly. Some of the origins are intrinsic to superconductivity [112]. Yip and Sauls were the first to point out that this nonlinearity in the Meissner effect reflects the symmetry of the pair wavefunction [113]. They suggested that λ changes linearly in magnetic field in a d-wave superconductor, in contrast to the conventional superconductor. Physically, this is due to the backflow of the quasiparticles. Thus, the magnetic field dependence of λ can be a new tool to study the symmetry of the pairing function.

Maeda *et al* measured $\lambda(H)$ of BSCCO [114] (and also of YBCO [115]), and found H-linear behaviour of λ, which was consistent with the prediction of Yip and Sauls for d-wave superconductivity. In this study, magnetic field was applied perpendicular to the CuO_2 plane, despite possible problems related to the large demagnetization factors and sharp edges. This was because it was the only possible configuration to catch λ_{ab} in BSCCO. However, this might cause field inhomogeneity, which is unfavourable for the magnetic-field dependence study. Subsequent studies with better resolution in samples where edges were rounded, and in the $H \parallel ab$ configuration [31, 116], found different results in YBCO from the previous results and also from the theoretical prediction. From the experimental point of view, a main problem for the field dependence measurement of λ is the presence of sharp edges of the crystal used, which possibly cause inhomogeneous current distribution. Thus, Bidinosti *et al* [116] prepared crystals where the edges were polished to a round shape.

For electron-doped NCCO, Maeda *et al* [117] measured $\lambda(H)$ in crystals formed into a circular disc shape. Although the temperature dependence of λ is apparently thermally activated, as was discussed above, the field dependence is consistent with the Yip–Sauls prediction, suggesting the presence of line nodes in the gap.

Recently, Jujo [118] re-investigated the Yip–Sauls result theoretically, and found a similar result to the experimental result of Bidinosti *et al* by treating the gauge invariant problem correctly. If any subsequent theories verify this conclusion, the field-dependence study of the cuprate superconductor can form a consensus.

To sum up, although the field dependence of λ could be a new, important method to discuss the symmetry of the condensate wavefunction, many issues remain to be seen, both experimentally and theoretically.

4.3. In-plane conductivity of quasi-particles in the superconducting state

To extract conductivity data of high-T_c cuprate, from the raw data (R_s and X_s), the most important problem is how to estimate the residual surface resistance, R_{res}, in the low-temperature limit [119]. R_{res} strongly depends on the sample quality [120], and may also depend on temperature in an unidentified way. Furthermore, for a d-wave superconductor, it is proposed theoretically [65, 121] that even an ideal sample exhibits an intrinsic residual conductivity, σ_{00}, of

$$\sigma_{00} = \frac{ne^2}{m}\left(\frac{\hbar}{\Delta_0}\right), \tag{24}$$

where n and m are the density and the effective mass of the electron, respectively. This corresponds to the residual surface resistance R^0_{res} of the order of $R^0_{res} \sim 5\times10^{-8}(\omega/2\pi)^2\ \Omega$ for

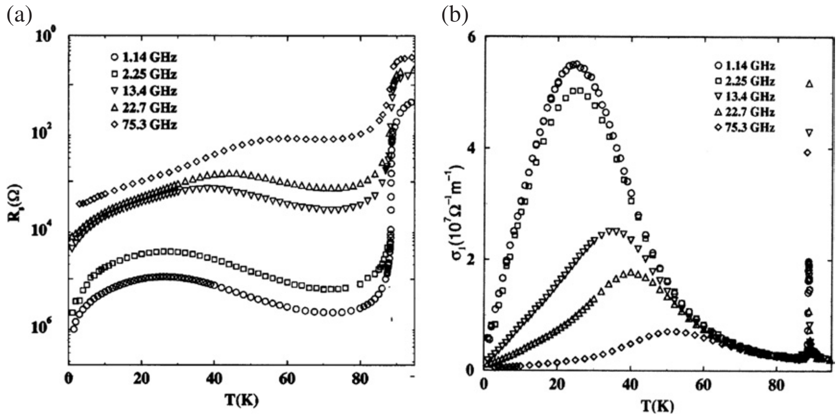

Figure 4. (a) Temperature dependence of R_s of YBCO. (b) Temperature dependence of the real part of the conductivity of YBCO at several microwave frequencies [52].

typical high-T_c cuprate superconductors, where $\omega/2\pi$ is the frequency in GHz [9]. Therefore, one should always keep in mind that very detailed quantitative discussions of σ at low temperatures in the superconducting state might be dangerous, unless complete knowledge about $R_{res}(T)$ has been obtained. Probably, the most satisfactory way of treating this problem is preparing superior crystals with very small R_{res} values. To the best of our knowledge, however, such crystals have been available only for YBCO [77]. In other most cases (or even for the crystals of 'high quality'), we should recall that how we treat R_{res} affects the extracted conductivity data seriously.

Figure 4(a) shows the in-plane surface resistance, R_s, of optimally doped YBCO crystals as a function of temperature, measured at five different microwave frequencies [52]. Two features are remarkable [9]. One thing is that a very low value of R_s (<1 mΩ at 22 GHz) was achieved, and the other thing is that the temperature dependence of R_s is nonmonotonic for such low-R_s crystals. Although the R_{res} value in the data of figure 4(a) is still larger than the intrinsically expected value, R^0_{res}, for a d-wave superconductor, Hosseini *et al* regarded that most of the R_{res} came from an intrinsic origin, and proceed further. To see what is going on more clearly, they obtained σ_1 from the R_s data as

$$\sigma_{ab} = R_s\left(\frac{2}{\mu_0^2\omega^2\lambda^3(T)}\right), \tag{25}$$

which is valid in the most temperature region of the superconducting state, where $\sigma_1 \ll \sigma_2$. Since they used $\lambda(T)$ data obtained in different measurements, they avoided various problems associated with the measurement of the reactive part, X_s.

Figure 4(b) shows the in-plane conductivity, σ_{ab}, of an optimally doped YBCO crystal as a function of temperature [52]. The most prominent feature in figure 4(b) is a large, broad hump below T_c. At first glance, the reader might think that this corresponds to the so-called coherence peak. However, it has been well established that there is no coherence enhancement in the temperature dependence of the longitudinal relaxation rate of nuclear spin, T_1^{-1}, measured by the NMR technique [122]. Since the measurement frequency is much lower in the NMR than in the microwave conductivity, a sharper, larger peak should show up in the NMR data, provided that the broad hump in figure 4(b) is the coherence enhancement. Thus, the broad hump in the microwave conductivity should be interpreted in terms of different origins other than the coherence enhancement.

Now, the structure has been interpreted as the result of the strong suppression of the QP scattering rate in the superconducting state [123–125]. The QP conductivity, σ_1, can be written as $\sigma_1 = n_{QP}e^2\tau/m^*$, where n_{QP}, τ, and m^* are the QP number density, scattering time, and effective mass of the QP, respectively. Since n_{QP} decreases and τ increases with decreasing temperature, a peak will show up in the temperature dependence. This suggests an electronic origin for the pairing mechanism of superconductivity, since the gap opening in the QP excitation spectrum can strongly suppress the QP scattering in the superconducting state. A similar conclusion, that the QP scattering time, τ, becomes longer in the superconducting state, was also obtained by thermal conductivity measurement [126].

As we mentioned briefly at the beginning of this subsection, the low-temperature behaviour of $\sigma_1(T)$ is strongly dependent on how one estimates the residual $R_{res}(T)$. Since the measured R_{res} is still higher than the ideal value even for the d-wave case, one should discuss the validity or the consistency of the above results. Hosseini *et al* discussed the frequency dependence (spectrum) of σ_1 from the data in figure 4(b) based on the two-fluid model, and found that (1) the data at each temperature were well fitted by the Drude formula,

$$\sigma_D \equiv \sigma_{dc}\frac{1}{1+(\omega\tau)^2}, \tag{26}$$

(2) the fitted τ increased with decreasing temperature very rapidly indeed, and (3) the temperature dependence of the spectral weight of the normal fluid $\int \sigma_1(\omega)\,d\omega$ agreed with that obtained independently form the penetration depth data, $1-(\lambda(0)/\lambda(T))^2$. This strongly suggests that the above analysis and the obtained conclusion are correct, as far as the data in YBCO are concerned.

Bonn *et al* investigated the effect of disorder in Zn and Ni doped YBCO [50]. They found several remarkable differences between Zn-doped and Ni-doped crystals, and ascribed them to the difference between the unitary scatterer (Zn) and the Born scatterer (Ni). Hirschfeld *et al* [65, 88] analysed their data in terms of a phenomenological d-wave model that treats strong scattering, and succeeded in explaining most of these results, including the temperature, and frequency dependences of conductivity, effect of disorder, etc. These were discussed in the review by Bonn and Hardy [9]. The only controversy between the experimental data and the theoretical interpretation in terms of the d-wave strong scattering theory was in the temperature dependence of σ_1 at low temperatures. As has already been mentioned, theoretically, it was expected that $\sigma_1 \propto T^2$, independent of the details of the models, because the QP density changed linearly in T and τ also changed linearly in T. On the other hand, the experimentally observed conductivity behaved as $\sigma_1 \propto T$. This discrepancy had been a puzzle. Recently, Turner *et al* [41] measured the conductivity spectrum between 0.6 and 20 GHz by the broadband bolometric method, and found a cusp-shaped conductivity spectrum, which was expressed as $\sigma_1(\omega, T) = \sigma_{dc}/[1+(\omega/\Gamma)^y]$, where a parameter Γ varied almost linearly in T, and $y \sim 1.45$. This means that σ_1 did not change linearly in T in the measurement with the improved sensitivity. Also theoretically, the inclusion of the order parameter suppression at impurity sites reproduced the $\sigma_1(T)$ data in [41] very well [127]. Thus, so far as the data in YBCO are concerned, it seems that almost all the aspects were consistent with the d-wave scenario. In particular, quantitative aspects were well explained by the strong-scattering theories. However, it should be recalled again that subtle behaviours at low temperatures are always linked to the possible extrinsic $R_{res}(T)$. In this method, although a possible uncertainty in $R_{res}(T)$ arising from the deviation of the sample σ_1 from an infinite σ_1 of a perfect conductor is eliminated, uncertainties arising from incomplete knowledge of the $R_{res}(T)$ of the sample itself cannot be eliminated. It is dangerous to rely on the $\sigma_1(T)$ behaviour too quantitatively, particularly at low temperatures.

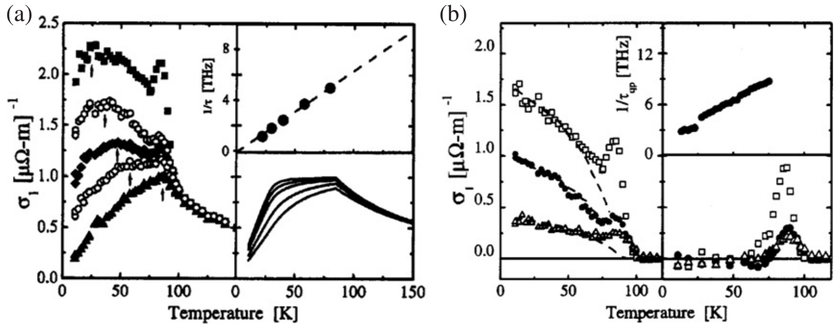

Figure 5. (a) Left panel: σ_1 of BSCCO plotted versus T for 0.2, 0.3, 0.4, 0.6, and 0.8 THz as squares, octagons, diamonds, circles, and triangles, respectively. Upper right panel: $1/\tau_{QP}$ as a function of temperature. Lower right panel: Drude conductivity, $\sigma_D(T)$ using τ_{QP} in the upper right panel [131]. (b) Left panel: σ_1–σ_D plotted at 0.2, 0.36, and 0.64 THz as squares, circles, and triangles, respectively. The dashed lines show the contribution of a collective mode. Lower right panel: the difference between the data and the fit. This was ascribed to thermal fluctuations. Upper right panel: $1/\tau(T)$ for the QPs [131].

In-plane anisotropy was reported by the same group [128]. They suggested that the *b*-axis conductivity can be adequately described by the sum of a Drude form, which is attributed to the thermally excited QP transport from quasi-two-dimensional bands, and a frequency independent background associated with a quasi-one-dimensional band. Thus, it seems that the underlying behaviour of the CuO_2 plane is strong, despite the presence of the one-dimensional CuO chain.

As we described above, for other materials than YBCO, a large R_{res} hindered a detailed analysis for conductivity. However, essentially the same behaviours were obtained for other materials such as BSCCO [119] and $La_{2-x}Sr_xCuO_4$ (LSCO) [129], by subtracting R_{res} (assumed to be T independent) before calculating σ_{QP} by equation (8).

Lee *et al* [53] measured R_s of crystals with lower R_{res} grown by Mochiku *et al* [130]. Since their R_{res} showed an ω^2 dependence, together with the T-linear $\lambda(T)$, they thought that their R_{res} was dominated by an intrinsic origin, and performed a similar analysis for the R_s data as was made in YBCO by Hosseini *et al*. As a result, their σ_1 remained higher than that in the normal state even in the low-temperature limit. This $\sigma_1(T)$ behaviour was essentially the same as was obtained by Shibauchi *et al* previously [119], when the residual R_{res} was not subtracted. Thus, the problem is, again, how one should interpret R_{res}. Although the ω^2 dependence of R_{res} is the same as the intrinsic BCS behaviour (equation (20)), the same frequency dependence can be caused by various extrinsic factors [120]. Indeed, many early R_s data of films with rather high value of R_s exhibited the ω^2 dependence. Thus, although progress was made in the sample quality, the intrinsic $\sigma_1(T)$ of BSCCO remained to be seen, even after the work by Lee *et al*.

Recently, $\sigma_1(T, \omega)$ data were taken by a rather different technique of THz transmission by Corson *et al* [131]. This technique is, at least, free from 'the residual R_s problem' in the microwave cavity perturbation technique, although different 'residual' problems may appear. They investigated the complex conductivity of the sample between 0.2 and 0.8 THz by measuring the complex transmission of the sample films. They found that σ_1 in the low-temperature limit decreased with increasing frequency (see figure 5). In other words, with decreasing frequency, σ_1 became higher than that above T_c, which was in agreement with what was obtained in many microwave measurements of samples with a finite R_{res}. This strongly suggests that R_{res} in microwave measurement does have some significance, and that it should be taken into the analysis. The authors considered that the two-fluid model was insufficient, and they added a third extra component which will be discussed later. Regarding that the QP contribution was represented by the Drude formula, as was made in YBCO, they found that the QP scattering rate underwent a T-linear behaviour even below T_c without showing any distinct discontinuity at T_c, which was found to be very different from what was established in YBCO. However, the T-linear behaviour of the scattering rate is in good agreement with a recent ARPES result for the QP in the nodal direction $((\pi, \pi))$ [132, 133]. With these results taken into account, the authors ascribed the large σ_1 even at the lowest temperatures to the third additional contribution for the dissipation which exhibits a similar temperature dependence to that of the superfluid density. They argued that this additional contribution was due to the order parameter fluctuation arising from the spatial inhomogeneity of the superfluid density, and that it could be caused by the same inhomogeneities that generated the different temperature dependence of the scattering rate from that in YBCO. The different behaviour of the QP scattering rate between YBCO and BSCCO may be related to the degree of inhomogeneity which generates the additional dissipation. A similar tendency was also observed in the increase of the QP τ inferred from the thermal conductivity data [61, 134]. Detailed systematic experiments of $\sigma_1(T, \omega)$ in various classes of materials with superior quality (in particular, the very small R_{res}) are still needed to clarify the above-mentioned conjecture.

To incorporate with these apparently inconsistent results, it is important to recognize the anisotropy of QP parameters in the Brillouin zone [135]. It is now becoming common sense that the Fermi surface development upon doping is nonuniform in k space [136]. Thus, we should identify the point in k space to discuss the QP behaviour. Also in an STM measurement on BSCCO [137], it was suggested that the superconducting property in the real space was nonuniform in the nano-scale. Thus, what kind of QP is probed in the transport experiment, and what kind of effect the disorder gives on the QPs, are subtle and unresolved problems. Recently, Gedik *et al* [138] tried to measure the QP scattering time τ of YBCO in the antinodal direction of the d-wave superconducting gap. Since it is difficult to probe antinodal QPs in the equilibrium condition, they used the transient grating technique, and measured the QP τ as a function of temperature, T, and the nonequilibrium current I. They found that τ was shorter than what was obtained by Bonn *et al* by more than two orders of magnitude. However, τ was found to diverge with decreasing T and I, which was explained by the momentum conservation in the electron–electron scattering. The validity of such a conservation law must be sensitive to disorder. Thus, in more disordered samples, we expect τ behaves in a very different manner. This may resolve the above-mentioned discrepancy in $\tau(T)$ of YBCO and BSCCO.

4.4. Anisotropy, interplane dynamics

As was pointed out at a very early stage, the electronic structure of high-T_c cuprates is quasi-two-dimensional (2D). For example, in the normal state, the in-plane (ab-plane) conductivity $\sigma_{ab}(T, \omega)$ is metallic, while the out-of-plane (c-axis) conductivity, $\sigma_c(T, \omega)$, is semiconducting [139]. This striking 2D nature is related to the exotic concept of the ‘charge confinement’, which was fundamental to the so-called non-Fermi-liquid model [140]. On the other hand, the so-called ‘cold-spot’ theory in the framework of the Fermi liquid model has also been proposed to explain such an unusual anisotropic property of the charge transport [135]. Thus, the strong anisotropic nature of the high-T_c cuprates has attracted much attention, since it is one of the central key issues associated with the mechanism of high-T_c superconductivity. In this subsection, we discuss this issue in the superconducting state, particularly focusing on the question of whether such strange quasi-2D properties in the high-T_c cuprates are maintained

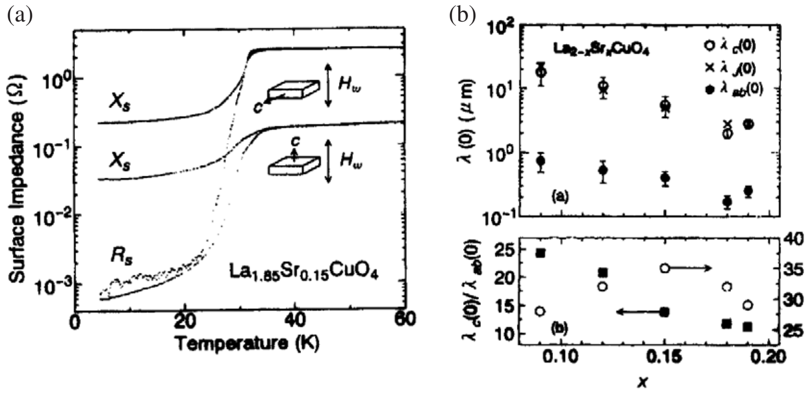

Figure 6. Anisotropy of (a) the surface impedance, and (b) the penetration depth of LSCO [86].

in the superconducting state or not. In addition, we will also review several methods to extract λ_c and σ_c.

4.4.1. Anisotropic superfluid reponse. The first systematic study of the anisotropic surface impedance of high-T_c cuprates was performed by Shibauchi *et al* [86]. They succeeded in measuring the penetration depth in both directions, λ_{ab} and λ_c for wide range of carrier concentration in LSCO (see figure 6(b)), by using the two kinds of configuration ($\mathbf{H}_\omega \parallel c$, $\mathbf{H}_\omega \perp c$). Note that the screening current flows in the CuO_2 planes in the configuration of $\mathbf{H}_\omega \parallel c$, while it flows in and across the CuO_2 planes in the configuration of $\mathbf{H}_\omega \perp c$. Z_s for each configuration is roughly described by Z_s^{ab} and Z_s^c as follows.

$$Z_s^{H_\omega \parallel c} = Z_s^{ab}, \tag{27}$$

$$Z_s^{H_\omega \perp c} = \frac{L_{ab} Z_s^{ab} + L_c Z_s^c}{L_{ab} + L_c}. \tag{28}$$

Here L_{ab} and L_c are the sample dimensions in the *ab* plane and in the *c* direction, respectively. Thus, Z_s^c can be obtained from equations (27) and (28). As shown in figure 6(a), two crystals with large faces parallel and perpendicular to the *ab* planes were prepared in order to minimize the difference of the demagnetizing factor.

They found that the Josephson-coupled layer model, which was originally suggested by Lawrence and Doniach (LD model) [141], successfully explained the magnitude of $\lambda_c(0)$ for a wide range of carrier concentration, and also that the overall temperature dependence of the superfluid fraction along the *c* axis was different from that in the *ab* plane, rather similar to the Ambegaokar–Baratoff [142] form of Josephson supercurrent. These results strongly suggest that superconductivity of cuprates should be described as a stack of 2D superconducting layers such as the LD model, rather than the anisotropic GL model.

Bonn *et al* [91] and Hosseini *et al* [143] measured $\lambda(T)$ in various directions of an untwinned YBCO crystal. In contrast to an LSCO crystal, since the contribution of Z_s^c to equation (28) was very small for a thin platelet crystal of YBCO (typically, $L_c/L_{ab} \sim 0.02$), they proposed to cleave a slab crystal into a set of narrow needles. This method can also avoid the problem of the changes of the demagnetizing factors between $\mathbf{H}_\omega \parallel c$ and $\mathbf{H}_\omega \perp c$ for the thin platelet sample. The difference between Z_s for n needles at $H_\omega \parallel a$ and that for the slab piece must depend only on Z_s^c as follows.

$$Z_s^{H_\omega \| a}(n \text{ needles}) - Z_s^{H_\omega \| a}(\text{slab}) = \frac{L_b Z_s^b + n L_c Z_s^c}{L_b + n L_c} - \frac{L_b Z_s^b + L_c Z_s^c}{L_b + L_c}$$
$$\approx (n-1)(L_c/L_b) Z_s^c. \tag{29}$$

Here, the final approximation is applied for the thin crystal ($L_b \gg L_c$). Although it seems that this method results in a poorly controlled inaccuracy due to nonideal cleaving, Hosseini *et al* reported that thin crystals with the best quality of detwinned YBCO cleave very cleanly in the [100] and [010] directions. They found that $\Delta\lambda_c$ is rather flat (roughly $\sim T^2$) at low temperatures, while the T linear behaviour was seen in $\Delta\lambda_a$ and $\Delta\lambda_b$. The T^2 behaviour in λ_c has been seen in LSCO [86], YBCO [91, 94, 143], and BSCCO [144], remarkably independent of a wide range of materials with different anisotropies.

In order to explain this T^2 behaviour such that it is consistent with the d-wave nature which was almost established in λ_{ab} measurement, it is necessary to consider the tunnelling (or hopping) process along the c axis in detail. For example, if the tunnelling or hopping process is purely coherent, independent of the in-plane momentum ($k_\|$), $\Delta\lambda_c(T)$ must agree with $\Delta\lambda_{ab}(T)$ [145]. Here, the term 'coherent' means that $k_\|$ is conserved in the tunnelling (or hopping) process. On the other hand, if it is purely incoherent, independent of $k_\|$, the resultant supercurrent along the c axis is zero, because of the vanishing average of the d-wave symmetry on the Fermi surface [146]. Thus, it is strongly suggested that the tunnelling (or hopping) process should be dependent on $k_\|$, whether it is coherent or incoherent.

In the framework of the Fermi-liquid theory, the most possible source of the T^2 behaviour is the incoherent impurity-assisted hopping, which was originally discussed by Radtke *et al* [145]. They showed T^2 behaviour in λ_c, by assuming the special form of the impurity-assisted hopping. Hirschfelt *et al* has also discussed a similar impurity-assisted hopping model, which gave rise to T^3 behaviour in λ_c in the clean limit and crossed over to T^2 behaviour at a temperature in the dirty limit [147]. Another possibility is the coherent direct hopping which is strongly dependent on $k_\|$. For a tetragonal cuprate, the band calculation suggests that the interlayer hopping integral has the form of $\propto[\cos(k_x) - \cos(k_y)]^2$, which vanishes along the nodal line of the $d_{x^2-y^2}$-wave order parameter [148]. This anisotropic hopping integral was applied to the cold-spot theory, and succeeded in explaining the behaviour of the c-axis dc and optical conductivity in the normal state [135, 149]. Xiang and Wheatley applied it to the superconducting state, and found that it gave rise to T^5 behaviour in λ_c at low temperatures [150]. Such weaker temperature dependence has been reported for the grain-aligned powders of $HgBa_2CuO_{4+\delta}$ [16] and the slightly underdoped single crystal of BSCCO [43]. However, as was discussed by Xiang and Wheatley, T^5 behaviour was observable only in clean tetragonal cuprates, and was easily replaced by T^2 behaviour due to the disorder effects, which were non-negligible in real materials. Thus, it seems that the observation of T^5 behaviour is almost impossible. The very flat behaviour observed in [16, 43] might have another origin.

On the other hand, in the framework of the non-Fermi-liquid model, the interlayer pair tunnelling model, which was originally proposed as the mechanism of high-T_c superconductivity [151, 152], has shown behaviour similar to T^2 behaviour in λ_c [153]. However, the coupled two-gap system assumed in [153], such as the planar and the chain layers in YBCO systems, is not a universal feature in high-T_c cuprates. In addition, the key assumption in the original model that the Josephson coupling energy is equal to the superconducting condensation energy has also been found not to be universal, by estimating the magnitude of λ_c of $Tl_2Ba_2CuO_{6+\delta}$ [154] and of $Bi_2Sr_2CuO_{6+\delta}$ [43].

To sum up, it seems that the universal T^2 behaviour in λ_c at low temperatures can be explained successfully in the framework of Fermi-liquid theory, by using the model of the incoherent impurity-assisted hopping mechanism.

As has been described in section 4.2, very recently, Hosseini *et al* investigated the doping and temperature dependence of λ_c at ~22.7 GHz [94], by using high-purity and homogeneous YBCO crystals with carrier concentration x near the boundary region between the antiferromagnetic insulators (AFI) and the d-wave superconductors (dSC) [155]. Instead of the cleaving method given by equation (29), they measured a thicker sample ($L_a \times L_b \times L_c = 1.803 \times 0.203 \times 0.391$ mm^3) in the configuration of $H_\omega \parallel a$. Since λ_c was very large for the heavily underdoped YBCO, comparable to L_b even at the lowest temperature (~1.2 K), they used an approximating formula,

$$\Delta f/f_0 = -\Gamma[1 - 2\tilde{\delta}/d \tanh(d/2\tilde{\delta})], \tag{30}$$

where $\tilde{\delta}$ was the effective screening length including the contribution of the displacement currents, and d was the sample thickness. Equation (30) can be obtained from the calculation of the complex eddy-current loss for a slab sample, ignoring the contribution of the supercurrent in the b direction [18, 156]. Thus, it is probably valid only for the region near SDR, although it seems to be possible to connect the SDR with the DPR continuously. Note that $\lambda_c(T)$ extracted from equation (30) is very sensitive to the change of the ratio λ_c/L_b, and that the Hagen–Rubens relation given by equation (11) is no longer effective for determining the magnitude of λ_c. Instead, they used an experimental result that $\Delta f/f_0$ was nearly independent of temperature at higher temperatures where the fields completely penetrated the sample. This was the same as already used by Shibauchi *et al* for the determination of λ_c of $La_{1.91}Sr_{0.09}CuO_4$ [86]. They found that not only the temperature dependence of ρ_s^c ($=1/\lambda_c^2$) but also the doping dependence were nearly quadratic, $\rho_s^c \approx ax^\alpha - bT^\alpha$ ($\alpha \sim 2$).

Sheehy *et al* [95] tried to explain these results by considering the effect of the QP charge renormalization phenomenologically, which was originally introduced by Ioffe and Millis [157]. They assumed that such a renormalization factor, Z_k, is vanishingly small for states away from the nodes of the d-wave pair potential, but close to unity in the vicinity of the nodes, and that the size of the area where $Z_k \approx 1$ scales with x, in a similar manner to the evolution of 'Fermi arc' (ARPES) with increasing x [136]. They found that the anisotropic shape of the Fermi arc in the $k_x k_y$ plane made the matrix element of the impurity-assisted hopping anisotropic more naturally, without using the special form proposed by Radtke *et al*. In addition, their model could also explain the behaviour of ρ_s^{ab} ($\rho_s^{ab} \approx ax - bT$), as discussed in section 4.2. This strongly suggests that the strength of superconductivity ($\propto \rho_s$) in the underdoped region is governed by the nodal QPs surviving to the boundary region between AFI and dSC.

4.4.2. Inter-plane conductivity of quasi-particles in the superconducting state. The first study of σ_1^c in the superconducting state was reported for YBCO by Kitano *et al* [158] and Mao *et al* [159], independently. Both groups measured both Z_s^{ab} and Z_s^c at ~10 GHz by using a similar method to Shibauchi *et al* (see equations (27) and (28)). It is important to note that equation (28) crucially requires the large size of L_c to determine R_s^c, since the anisotropy of R_s can become much smaller than that of X_s (or λ), as shown in figure 6(a). Thus, the results by Kitano *et al* seem to be more reliable, since they used very thick crystals ($L_c = 0.4$–0.9 mm, $L_c/L_{ab} \sim 1$). Such thick crystals also have an advantage to reduce the difference of the demagnetizing factor between $H_\omega \parallel c$ and $H_\omega \perp c$.

Kitano *et al* reported that the temperature dependence of $\sigma_1^c(T)$ of a nearly optimally doped YBCO ($T_c = 93$ K) (sample A) showed a broad peak similar to that of $\sigma_1^{ab}(T)$, suggesting that

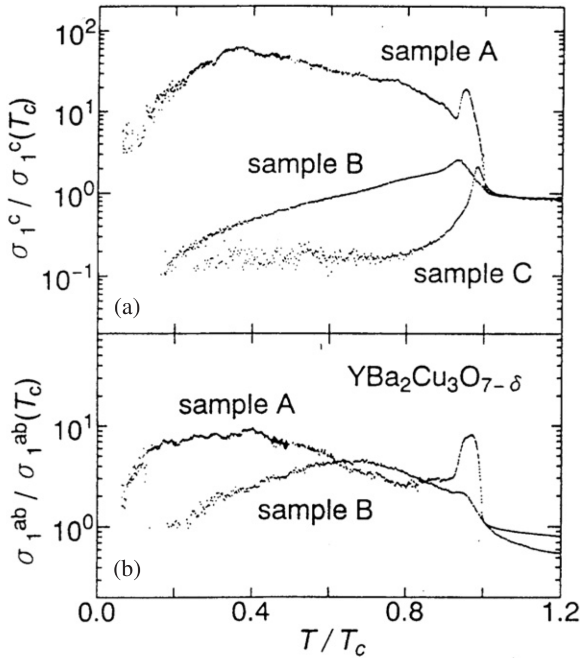

Figure 7. QP conductivity, σ_1, of YBCO both (a) in the c direction and (b) in the ab plane [158]. T_c values are 93 K, 65 K, and 63 K for samples A, B, and C, respectively.

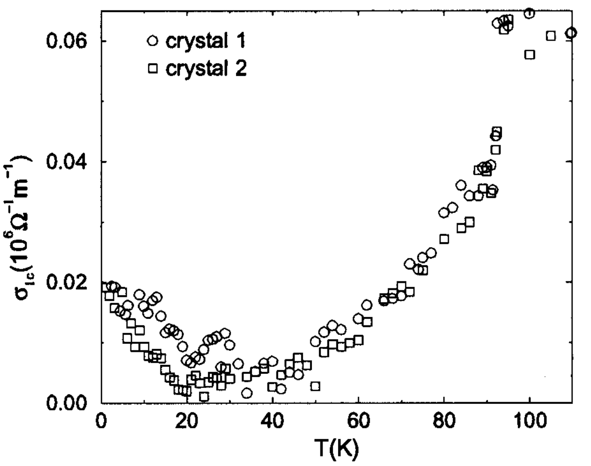

Figure 8. Temperature dependence of σ_c of YBCO [143].

the QP scattering became less anisotropic below T_c (figure 7). They also reported that $\sigma_1^c(T)$ for the underdoped YBCO ($T_c = 65$ and 63 K) (samples B and C) did not show the peak below T_c, suggesting that the QP dynamics for underdoped cuprates kept the strong 2D nature even in the superconducting state.

On the other hand, Hosseini *et al* measured R_s^c of the optimally doped YBCO at 22 GHz by using the cleave method as was described in equation (29) [143]. They reported that R_s^c obtained from equation (29) was so small that the resultant $\sigma_1^c(T)$ fell rapidly below T_c, and rose slightly below 20 K, with no sign of the peak as observed in [158] (figure 8).

The origin of the discrepancy between the data in [158] and those in [143] has not been resolved yet. As already described, in [158] thick crystals ($L_c/L_{ab} \sim 1$) were used, and the change of the demagnetizing factors was not important. The uncertainty due to the change in the *ab*-plane current distribution was comparable to their previous study on LSCO [86], and was also found to be unimportant. It is worth noting that, recently, Nefyodov *et al* [160] reported a similar result to that in [158], by measuring a rectangular crystal ($L_a \times L_b \times L_c = 0.4 \times 1.6 \times 0.1\ \mathrm{mm}^3$) of the optimally doped YBCO grown in a BZO crucible. They also calculated the geometrical factor in the configuration of $H_\omega \parallel c$, by applying the conformal mapping method to a long strip with rectangular cross section in order to include the demagnetization effect correctly. According to their calculation, the difference of the demagnetizing factors was within an order of magnitude even for the ratio of $L_c/L_{ab} \sim 0.01$.

Concerning the controversy, it may rather be the case that the use of thin crystals ($L_c/L_b \sim 0.02$) in [143] makes the extraction of R_s^c much more difficult. In addition, equation (29) assumes that the contribution of $L_b R_s^b$ to $R_s^{H_\omega \parallel a}$ is not changed between before and after the sample cleaving. This assumption can be violated easily by the nonideal sample cleaving. For thin crystals with $L_c \ll L_b$, the uncertainty due to this change may be comparable to $(n-1)L_c R_s^c$, which can be an important origin for the error.

Another important point is that the behaviour of σ_1^c is dependent on the oxygen content [158]. The systematic optical study of YBCO crystals with various oxygen contents also clarified that a Drude-like feature was observed in σ_{opt}^c below 200 cm^{-1} for the slightly overdoped sample in the superconducting state, while there was no such sign for the underdoped and optimally doped samples [161, 162]. Indeed, in contrast to Hosseini *et al*, the overall temperature dependence of superfluid fraction in [158, 160] was found to be isotropic, suggesting isotropic coherent charge transport. As was discussed by Xiang and Hardy [163], the formation of the CuO chains with increasing oxygen content reduces the crystal symmetry so that the interlayer hopping transfer remains finite along the nodal line of the $d_{x^2-y^2}$ order parameter. This effect leads to the coherent charge transport along the *c* axis. Thus, the discrepancy between these data may be due to a small difference in the oxygen content.

It is well known that BSCCO exhibits the strongest anisotropy ($\sigma_{\mathrm{dc}}^{ab}/\sigma_{\mathrm{dc}}^c \sim 10^5$) among all the high-$T_c$ cuprates. This material has the advantage that there is no extra contribution to the *c*-axis charge transport other than the excited carriers in the CuO_2 planes. Although the measurements were previously performed to obtain Z_s^c of this material in the configuration of $H_\omega \perp c$ [79, 80], it is almost impossible to obtain Z_s^c by this method, since λ^c of BSCCO is very large (∼100–500 μm), almost comparable to L_{ab}. Thus, the assumption of the skin depth regime (SDR) is no longer valid, and new methods are required.

Kitano *et al* [164] succeeded in obtaining $\sigma_1^c(T)$ by regarding that the sample was in the depolarization regime when it was measured at $E_\omega \parallel c$. They measured the complex dielectric constant, $\epsilon(T)$, for the slightly underdoped BSCCO ($T_c = 87$ K) at 50 GHz by using equation (12), and found that $\sigma_1^c(T)$ showed a sudden drop just below T_c and a large increase below ∼0.9 T_c [165]. One possible source of the increase was a misalignment effect. However, it is probably not important, since a heavily underdoped $Bi_2Sr_2Ca_{0.8}Y_{0.2}Cu_2O_y$ (BSCYCO) ($T_c = 52$ K) shows a monotonically decreasing $\sigma_1^c(T)$ with decreasing temperature [144]. They concluded that the behaviour of $\sigma_1^c(T)$ was dependent on the hole concentration, and that the large increase observed in the slightly underdoped BSCCO had an intrinsic origin. The origin of this anomalous behaviour has not been clarified yet. As a possible candidate, the dissipation in the stacked Josephson π junctions has been considered [166]. Another candidate is an excess conductivity caused by the spatial inhomogeneity of the superfluid density, which was considered for the interpretation of σ_1^{ab} by Corson *et al* [131]. As was described in the previous subsection, if this additional dissipation exhibiting a similar temperature dependence to that of the superfluid density contributes to σ_1^{ab}, it might also contribute to σ_1^c in a similar manner.

Another approach has been developed by Gaifullin *et al* [43]. They proposed that the c-axis QP conductivity, σ_{QP}^c, was proportional to the line width of the Josephson plasma resonance (JPR), based on a simple description using the two-fluid model. They measured the linewidth of JPR for the underdoped BSCCO ($T_{\mathrm{c}} = 82.5$, 77.2, and 68 K), and concluded that σ_{QP}^c remained suppressed to a small value even in the superconducting state, which was qualitatively similar to the result in BSCYCO [144]. This method has also been applied to the optical reflectivity measurements for $Tl_2Ba_2CuO_6$ and $Tl_2Ba_2CaCu_2O_8$ thin films [168]. However, it should be noted that the deduction of $\sigma_{\mathrm{QP}}^c(T)$ as a function of temperature in [43, 168] required the assumption that σ_{QP}^c was independent of frequency at least in the measured microwave (or infrared) frequency region, which has not been confirmed experimentally yet. In addition, Artemenko *et al* [167] have shown that such a simple relation between the JPR linewidth and σ_{QP}^c was valid only for the limiting temperature region near T_{c}, by calculating the dielectric function in the clean d-wave superconductors with $k_\parallel$-independent coherent interlayer tunnelling. This strongly suggests that the temperature dependence of the linewidth and plasma frequency of JPR should be analysed more carefully, and that the estimate of σ_{QP}^c by this method is invalid at low temperatures. In order to obtain σ_{QP}^c correctly, it is necessary to model the interlayer charge transport more exactly, which has not been performed yet.

The I–V characteristics of the c-axis intrinsic Josephson junctions in the slightly overdoped BSCCO have been investigated by Latyshev *et al* [169]. They proposed that σ_{QP}^c could be obtained from the differential conductance in the limit of the zero bias when all intrinsic junctions were resistive, and reported that σ_{QP}^c varied as T^2 below 30 K. However, it is necessary to re-examine the validity of their proposal. In fact, the I–V curve in the resistive state for conventional Josephson junctions does not always correspond to that of the QP tunnelling obtained by suppressing superconductivity with a sufficiently strong magnetic field [170]. Thus, it seems difficult to remove the finite dissipative contribution of Cooper pair tunnelling from the I–V curve of the all-junction resistive state.

In summary, the experimental results of the interlayer conductivity of QPs in the superconducting state are still controversial, even now. However, at least for the underdoped materials, the behaviour of σ_1^c seems to decrease monotonically with decreasing temperature even in the superconducting state. In the framework of the Fermi-liquid theory, this behaviour is qualitatively consistent with the incoherent impurity-assisted hopping model [145] and the coherent cold-spot scattering model [163]. On the other hand, in any models based on the non-Fermi liquid, $\sigma_1^c(T)$ has not been calculated definitely yet. Such calculations are needed to take the discussion of $\sigma_c(T)$ further.

4.5. *Dynamical fluctuations of superconductivity in the microwave conductivity*

The effect of thermal fluctuation in conventional superconductors has been investigated mainly in the temperature region outside the 'critical regime', where the GL theory is expected to break down due to the strong fluctuation [171]. Aslamazov and Larkin (AL) [172] have microscopically derived the contribution of the excess dc conductivity above T_{c}, which is attributed to the Gaussian fluctuation of the amplitude of the order parameter.

$$\Delta\sigma_{\mathrm{AL}}^{\mathrm{3D}} = \frac{e^2}{32\hbar\xi(0)}\frac{1}{\epsilon^{1/2}}, \qquad \Delta\sigma_{\mathrm{AL}}^{\mathrm{2D}} = \frac{e^2}{16\hbar d}\frac{1}{\epsilon}, \tag{31}$$

where $\epsilon = (T - T_{\mathrm{c}})/T_{\mathrm{c}}$, $\xi(0)$ is the zero-temperature correlation length, and d is the thickness of the superconducting layers, respectively. Maki and Thompson (MT) pointed out that the pair breaking effect of QPs also contributed to the excess dc conductivity [173]. Thus, the total excess dc conductivity is given by the sum of the AL term and the MT term. Schmidt generalized the AL term for the ac conductivity above and below T_c by using the time-dependent Ginzburg–Landau (TDGL) theory [174], while the generalization of the MT term for finite frequencies has not been performed yet. Lehoczky and Briscoe [175] have investigated the fluctuation effect on the microwave conductivity of Pb thin films experimentally, and found that both the temperature and frequency dependences of the ac conductivity were in agreement with the calculation of Schmidt.

It is interesting to explore the superconductivity fluctuation *inside* the critical region. In conventional superconductors, however, it is known that the critical region was very small close to T_c, so that it cannot be accessed easily in experiments. However, after the discovery of high-T_c superconductivity, Fisher, Fisher, and Huse (FFH) [176] pointed out that the thermal fluctuation effect is greatly enhanced in high-T_c cuprates, because of the short coherence lengths, the high critical temperatures, and the strong 2D properties. This implies that the critical region may be observable experimentally. For strongly type-II superconductors, they predicted that the usual Gaussian regime described by the GL theory will cross over to a critical regime of a weakly charged superfluid where the fluctuation of the order parameter is described by the XY model. FFH also showed that, in such a critical regime, the ac fluctuating conductivity scales as

$$\sigma(\omega) \sim \xi^{2-d+z} S(\omega\xi^z), \tag{32}$$

where $S(x)$ is a complex universal scaling function of the scaled frequency $x \sim \omega\xi^z$, ξ is the correlation length diverging at T_c as $\xi \sim |T - T_c|^{-\nu}$, d is the dimensionality of the system, ν is the static critical exponent, and z is the dynamical critical exponent. Kamal *et al* [177] measured $\lambda_{ab}(T)$ of the optimally doped YBCO crystals, by using a split-ring resonator operated at 0.9 GHz, and showed that $\lambda(T)/\lambda(0) \propto \epsilon^{-y}$ with $y \approx 1/3$ over the wide range $10^{-3} < \epsilon < 0.1$. This result was excellently consistent with the critical behaviour of the 3D XY model with $\nu = 2/3$. They also confirmed that this critical behaviour was not affected by the presence of small amounts of Zn impurities, as suggested by FFH.

In high-T_c cuprates, it was established experimentally that a sharp peak showed up in the temperature dependence of $\sigma_1(T)$ at around T_c [9] (see also in figure 4(b)). Horbach and Saarloos [178] calculated the frequency-dependent AL term for 2D superconductors above and below T_c, using the results of Schmidt, and showed that a fluctuation-induced sharp peak appeared in $\sigma_1(T)$ just at T_c. Thus, the sharp peak in $\sigma_1^{ab}(T)$ attracted much attention, since it was possible that the critical fluctuations can be observed in it.

However, Olsson and Koch [179] pointed out that a distribution of T_c due to the sample inhomogeneity also caused a spurious peak in $\sigma_1(T)$ just *below* T_c. Anlage *et al* [180] measured $\sigma^{ab}(T)$ at 9.6 GHz of YBCO single crystals, which showed a clear T-linear behaviour in $\Delta\lambda_{ab}(T)$ at low temperatures. They concluded that the 2D AL term was quantitatively consistent with $\sigma_1^{ab}(T)$ for $\epsilon > 3 \times 10^{-3}$ above T_c, while the behaviour of $\sigma_1^{ab}(T)$ for $0 < \epsilon < 3 \times 10^{-3}$ was well described by an effective medium model, based on a Gaussian distribution of T_c. In particular, they found that this simple model reproduced all the experimental results very well, such as the peak height, the peak width, and the fact that $\sigma_1^{ab}(T_c) = \sigma_2^{ab}(T_c)$. These results suggested that the peak of $\sigma_1^{ab}(T_c)$ was not attributable to critical fluctuations at all. On the other hand, Waldram *et al* [181] came to an opposite conclusion by investigating $\sigma^{ab}(T)$ at 14, 25, and 36 GHz of BSCCO, $Tl_2Ba_2CuO_6$, and Zn-doped YBCO. They also analysed the peak of $\sigma_1^{ab}(T_c)$ using a similar effective medium model, although it was not based on the distribution of T_c, but on the conversion of normal current to superconducting current in the critical regime. Since Anlage *et al* analysed the data in terms of the T_c distribution, we should be informed about why the data in [181] could not be explained by the effective medium theory plus the distribution of T_c. However, we could not know these in [181]. We should always keep in mind that the effect of inhomogeneity often plays important roles in various aspects of the data in high-T_c cuprates. The peak of $\sigma_1^{ab}(T_c)$ should be analysed more carefully, together with more careful sample characterizations.

It is also noteworthy that the experimental 'fact' of $\sigma_1(T_c) = \sigma_2(T_c)$ reported in these papers might not be correct if a recent theory of Peligrad *et al* [182] is taken into account, which pointed out the importance of the short-wavelength cut-off effect in the ac fluctuating conductivity.

In addition, the asymmetric behaviour of the observed fluctuation above and below T_c (2D Gaussian type above T_c, while 3D XY type below T_c) also seems puzzling, since the critical behaviour is usually symmetric above and below the critical point. This suggests that the temperature dependence of $\sigma(T)$ at a fixed frequency alone is not enough to analyse the critical behaviour. Rather, both the temperature and frequency dependences of $\sigma(\omega, T)$ should be analysed using the scaling relation of equation (32). Dorsey [183] showed that the FFH result was reduced to the AL-Schmidt results in the mean field theory ($\nu = 1/2$, $z = 2$) for purely relaxational dynamics (the so-called 'model A' in the Hohenberg and Halperin classification [184]). He also argued that equation (32) should be correct even for a 2D Kosterlitz–Thouless (KT) transition (2D XY model) [185]. Wickham and Dorsey also showed that the scaling hypothesis of FFH was also verified for the relaxational XY model ($\nu = 2/3$, $z \approx 2$) [186]. Thus, the scaling relation (32) is valid for various theoretical models. At T_c, FFH showed that the magnitude $|\sigma|$ and phase ϕ of $\sigma(\omega)$ must scale as

$$|\sigma(\omega)| \sim c|\omega|^{-(2-d+z)/z}, \tag{33}$$

$$\phi_\sigma = \frac{\pi}{2}\left[\frac{2-d+z}{z}\right], \tag{34}$$

respectively.

As was described in section 3.1.2, the broadband technique developed by Booth *et al* is a very powerful probe to check the scaling relation (32) directly [46]. They measured the frequency-dependent $\sigma(\omega, T)$ (45 MHz–45 GHz) of YBCO thin films above T_c. They found that $\phi_\sigma \sim (\pi/2) \times (0.64 \pm 0.1)$ at T_c, which suggests $z = 2.65 \pm 0.3$ by assuming $d = 3$. The plots of both $|\sigma(\omega)|$ and $\phi_\sigma(\omega)$ for five different temperatures within 1 K above T_c were found to be put onto a single curve with the choice of $z = 2.65$, and $\nu = 1.0$. Although they succeeded in obtaining both the static (ν) and dynamic (z) critical exponents, the estimated values did not agree with the Gaussian behaviour ($\nu = 1/2$, $z = 2$) or the 3D XY behaviour with $\nu = 2/3$. The reason for such discrepancies remained unresolved.

Corson *et al* [187] discovered the contrasting behaviour in the underdoped BSCCO thin films in the frequency range between 100 and 600 GHz. They found that $\sigma_2(T, \omega)$ measured the phase-stiffness energy $k_B T_\theta$ ($\equiv \hbar\omega\sigma_2/\sigma_Q$) below T_c, where σ_Q ($\equiv e^2/\hbar d$) was the quantum conductivity of a stack of planar conductors with the interlayer spacing d. They showed that $T_\theta(\omega)$ was frequency independent below a crossover temperature, while it began to depend strongly on frequency above the crossover temperature. This feature is quite reminiscent of the phase-stiffness dynamics in the KT theory. Furthermore, the scaling behaviour of $\sigma(T, \omega)$ for the temperature range from 64 to 91 K ($T_c = 74$ K) and the frequency range from 100 to 400 GHz also suggested that the system is strictly 2D and the scaled frequency Ω depends exponentially on the inverse of the reduced temperature. These results strongly suggest that a very broad temperature region above T_c is governed by the 2D XY type of critical fluctuation.

In summary, it seems that the dynamic critical fluctuations have been observed in several experiments on $\sigma(\omega)$ study of the high-T_c cuprates. However, no consensus has been formed on the quantitative aspects, such as the numbers of critical exponents. Although the broadband techniques which can obtain $\sigma(\omega, T)$ is very powerful to explore the critical behaviour, only a few results have been obtained by this technique. To settle the above-mentioned controversy, more detailed information on $\sigma(\omega, T)$ in sufficiently characterized samples is crucial for various systems of high-T_c cuprates.

5. Flux flow and electronic structure of vortex core of cuprate superconductors

5.1. Flux flow and flux creep

In the so-called type-II superconductors, magnetic flux penetrates as quantized vortices above the lower critical field, B_{c1}.[6] Each vortex has the magnetic flux of $\Phi_0 = h/2e$, where Φ_0 is the flux quantum. Around the vortex, supercurrent circulates. In high-T_c cuprates, owing to the strong two dimensionality, the circulating current around the quantized vortex is confined in each CuO_2 plane (pancake vortices) [188]. When the magnetic field is applied parallel to the CuO_2 plane, we can have coreless Josephson vortices [189, 190].

Vortices move under the presence of driving current density, $\mathbf{j}$, since they suffer Lorentz force density, $\mathbf{f}_L$,

$$\mathbf{f}_L = \mathbf{j} \times \Phi_0. \tag{35}$$

When they move, energy is dissipated at the core (*flux flow*). Bardeen and Stephen (BS) [191] were the first to calculate the energy dissipation by the flux flow. They assumed that the core can be regarded as a normal metal, and found that the flux-flow resistivity, ρ_f, was ohmic, and was given by

$$\rho_f = \rho_n \frac{B}{B_{c2}}, \tag{36}$$

where ρ_n is the resistivity in the normal state[7]. In the presence of the vortex, equation (36) is added to the usual quasiparticle resistivity.

If there is finite pinning of a vortex, the reactive part appears in the resistivity. A simple equation of motion for the displacement of a vortex, $\mathbf{u}(\mathbf{r}, t)$ at the point $\mathbf{r}$, is

$$\eta\dot{\mathbf{u}} + \kappa_p \mathbf{u} = \mathbf{f} e^{i\omega t}, \tag{37}$$

where $\mathbf{f}$ is the driving force with the magnitude of $|\mathbf{j}|\Phi_0$, and

$$\eta = B\Phi_0/\rho_f \tag{38}$$

is the viscosity of the vortex; κ_p is a pinning constant. This gives the resistivity, ρ, as

$$\rho = \rho_f \left(\frac{1}{1 - i(\omega_p/\omega)} \right), \tag{39}$$

where

$$\omega_p = \frac{\kappa}{\eta} \tag{40}$$

is the crossover frequency that gives a crossover from the low-frequency reactive response to the high-frequency dissipative (resistive) response. This crossover was beautifully observed in conventional superconductors [193].

[6] In this section, different from the previous sections, we represent B, not H, by the term 'magnetic field'.
[7] Recently, Kita calculated the flux-flow resistivity of a clean conventional (s-wave) superconductor, and obtained that ρ_f is sublinear in B [192].

At finite temperatures, thermal energy plays an essential role, in particular in high-T_c superconductors. Thermal energy can make vortices escape from the pinning potential well (*flux creep*) [194]. Application of the driving current introduces the unbalance between the left going current and the right going current, and leads to the net creep velocity in one direction, causing a finite voltage.

When all of these effects plus the contribution of QPs to the complex surface impedance are included, simple analogies to the parallel or the series circuit are no longer valid. Within the framework of the mean-field treatment for the intervortex interaction, such a calculation was made by Coffey and Clem [195]. Their expression for the complex surface impedance has become a starting point of the analysis of the experimental data of the ac response in the mixed state, in many cases.

5.2. Microscopic electronic structure of vortex core in conventional superconductors

At the vortex core, the superconducting pair potential is weak. This means that there are bound states in the vortex core. According to an exact analysis by Carrori, de Gennes, and Matricon [196], a series of bound states exist, with their minimum energy of

$$E_{\min} = \frac{1}{2}\Delta E = \frac{1}{2}\frac{\Delta_0^2}{E_F} \equiv \frac{1}{2}\hbar\omega_0, \tag{41}$$

where ΔE is the level spacing, Δ_0 is half of the mean-field superconducting gap, and E_F is the Fermi energy; ω_0 is the crossover frequency defined in equation (40), and was found to be equal to the cyclotron frequency at the upper critical field, B_{c2}. For conventional superconductors (CSCs), $E_{\min}$ is of the order of 1–10 μeV, which is hardly resolved by any experimental techniques available [197]. Disorder introduces a finite lifetime $\tau \equiv \hbar/\delta E$ for these bound states, where δE is the level broadening. We can introduce an important microscopic parameter, Γ, defined as

$$\Gamma \equiv \frac{\Delta E}{\delta E} = \omega_0\tau, \tag{42}$$

that dominates the QP behaviour in the vortex core.

It is important to note that Γ determines the flux flow resistivity (or viscosity, see equation (38)). The vortex viscosity η, and the Hall viscosity α_H, were calculated [198, 199] for arbitrary values of $\omega_0\tau$ as

$$\eta = \pi\hbar n\frac{\omega_0\tau}{1+(\omega_0\tau)^2}, \tag{43}$$

$$\alpha_H = \pi\hbar n\frac{(\omega_0\tau)^2}{1+(\omega_0\tau)^2}, \tag{44}$$

where n is the QP concentration. In the dirty limit, as is usually the case ($\omega_0\tau \ll 1$), $\eta \simeq \pi\hbar n\omega_0\tau = B_{c2}\Phi_0/\rho_n$, which is the BS expression [191]. In the opposite limit, $\omega_0\tau \gg 1$ (superclean limit), the Hall effect dominates.

$$\rho_v = \frac{B\phi_0}{\eta + \alpha_H^2/\eta} \equiv \frac{B\Phi_0}{\eta_{\text{eff}}}, \tag{45}$$

where η_{eff} is the effective viscosity. This means that the viscosity, obtained in the experiment under the condition $\mathbf{j} = \text{const}$, was η_{eff}. Equation (45) can be rewritten as

$$\frac{\eta_{\text{eff}}}{\pi n\hbar} = \Gamma. \tag{46}$$

Therefore, we can determine the QP lifetime in the vortex core from the estimates of the viscosity of the vortex in the mixed state.

5.3. *Electronic states of vortex core of high-T_c superconductor*

5.3.1. General remarks. In HTSCs, the above-mentioned simple description of the vortex core is incorrect for several reasons. First, the energy gap has d-wave symmetry [85]. Since the amplitude of the gap at the node is zero, QPs are not localized in the vortex core but extended along the node direction [200]. A theoretical calculation suggested that there were no truly localized states in the vortex core in pure $d_{x^2-y^2}$ superconductors [201]. On the other hand, recent STM results in HTSCs showed that the DOS at a finite energy below the gap Δ_0 was enhanced near the centre of the vortex core [89, 202, 203]. Therefore, the presence or the absence of localized states in the vortex core of HTSCs is still one of the central basic questions.

The second characteristic feature of the vortex core in HTSCs is the semi-quantum nature of the core. Again, the STM results suggests that $k_F\xi \simeq 2$–3, where ξ is the GL coherence length, and k_F is the Fermi velocity [89, 202, 203]. This means that the quasiclassical approximation is no longer valid, and the physics of such a quantum core has not been developed up to now. In particular, in such a highly anomalous situation, to the best of our knowledge, there have been no rigorous calculations of the dynamic properties of vortices, in particular for d-wave superconductors. So, the appearance of new effects may be expected in the dynamics of vortices in HTSCs.

Within the framework of the quasiclassical approximation, Kopnin *et al* discussed the flux flow of a vortex in d-wave superconductors [204]. They found that an extra dissipation exists even for a superclean core. This means that equation (41) is not valid for the very clean core. Physically, this is due to the Landau damping of the QPs in the vortex core. Thus, care should be taken to analyse the flux flow data, even when they show a large dissipation for d-wave superconductors.

5.3.2. Experiments on viscosity measurement. There have been many experimental efforts to determine the vortex dynamics parameters of YBCO [10, 40, 51, 193, 205–208], and a review of earlier results was provided in [10]. Among them, a report of [40] caused a debate. Matsuda *et al* measured the microwave loss as a function of magnetic field up to 7 T at low temperatures, and deduced a very large viscosity, which was two orders of magnitude larger than in CSCs. This huge value was interpreted as evidence that the core of YBCO was in the superclean regime, $\omega_0\tau \gg 1$. However, their estimation of the viscosity was based on the assumption that the crossover frequency, ω_p, is much smaller than the measurement frequency, ω. Under that assumption, they estimated the viscosity only from the data of the surface resistance, R_s. In CSC, this assumption was reasonable since the characteristic crossover frequency $\omega_p \sim 100$ MHz [193]. In HTSC, however, the condition $\omega \gg \omega_p$ might not be satisfied. Indeed, experimentally estimated values of the crossover frequency ω_p at low temperatures in previous reports [10, 205, 207] were on the order of $\sim$10 GHz. In such a case, the estimation of $\eta_{\rm eff}$ from R_s alone leads to an incorrect result for η, and the measurement of Z_s as a complex quantity is essential.

To discuss the problem exactly, Tsuchiya *et al* [51] measured the complex surface impedance as functions of magnetic field, frequency, and temperature up to higher magnetic fields. Through the comparison with a theoretical calculation by Coffey and Clem [195], they estimated ω_p, η, and $\kappa = \omega_p\eta$ (figure 9). Estimated values of $\eta_{\rm eff}$ at 10 K are $\sim$4–5 $\times$ 10^{-7} N s m^{-2}. These values correspond to $\omega_0\tau \sim 0.3$–0.5. Since equation (42) can be rewritten as $\Gamma = (\pi/4)(1/k_F\xi)(\ell_{\rm core}/\xi)$ ($\ell_{\rm core}$ is the mean free path of the QP in the core), this means $\ell_{\rm core} \sim \xi$ (‘moderately clean’). The moderately clean nature of the vortex core was found to be generic to other cuprate superconductors such as BSCCO [209, 223] and

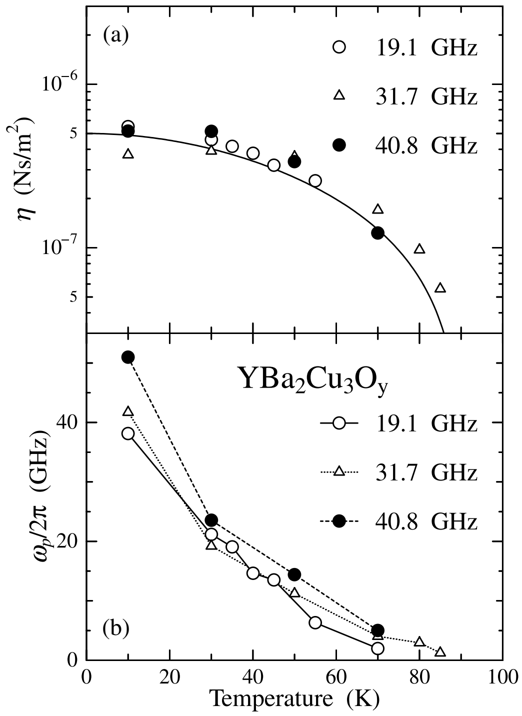

Figure 9. (a) Viscosity and (b) crossover frequency of YBCO obtained by the microwave surface impedance measurement [51].

LSCO [210]. There, the moderately clean nature was also found to be robust on carrier doping. It is worth noting that the direct measurement of the viscosity by applying a very high current pulse in YBCO [211]was also consistent with the moderately clean nature of the core.

This is in sharp contrast to the QP mean free path in the Meissner state, as was discussed in section 4, suggesting a rather different scattering mechanism dominates the QP in the core. For QPs in the vortex core, it was suggested that the Andreev reflection at the core boundary is important [199]. This mechanism might limit the mean free path of QP as $\sim\xi$.

Another significance of the moderately clean nature of the core is that a moving vortex dissipates large energy, even for $k_F\xi \sim 1$. On the other hand, the STM data suggest that almost no dissipation will take place because there were almost no QP states in the core. How to reconcile the moderately clean nature seen by microwave experiment and the extremely quantum nature seen by the STM experiments is a serious problem. To approach the problem, the introduction of disorder might be useful, since a definite difference was observed in the induced QP DOS in the Meissner state among Zn-doped and Ni-doped BSCCO [89]. In a recent viscosity measurement in impurity-doped YBCO, there was little difference in the microwave dissipation of the vortex core between Zn-doped and Ni-doped crystals [212]. This suggests that the QP DOS in pristine samples is rather large, so that the difference caused by Zn and by Ni is masked, which is inconsistent with the QP DOS inferred by the STM data. Thus, some revision might be necessary in the interpretation of the STM data. Alternatively, a quite new mechanism of dissipation might exist for the flux flow of the quantum core. Nobody knows about the dissipation of the quantum core, in particular, for d-wave superconductors. A fairly large dissipation observed in microwave experiments might suggest that a new physics lies behind the motion of a quantum core [213]. Recently, the existence of other related ordered structures, such as antiferromagnetism etc [214–218], was proposed in the vortex core. These should affect various aspects of flux flow, both qualitatively and quantitatively, and might resolve the above-mentioned discrepancy.

5.3.3. A new feature as superconductors with nodes in the gap. For anisotropic superconductors with nodes in the gap, new effects were found also in the flux flow. In a heavy electron suerpconductor, UPt_3 [219], and a boron-carbide superconductor, YNi_2B_2C [220], it was reported that the flux-flow resistivity, ρ_f, was enhanced at low fields, that means the dependence of ρ_f as a function of magnetic field, B, $\rho_f(B)$, showed an upward concave behaviour. Since these two materials are considered to be anisotropic superconductors with nodes, it is expected that the HTSCs also exhibit a similar behaviour. The data in YBCO [51] exhibited that ρ_f was proportional to B at low field. However, since an exact value of B_{c2} was unknown, it could not be concluded whether ρ_f was enhanced or not. Matsuda *et al* [221] investigated $Z_s(B)$ of the underdoped cuprate whose B_{c2} could be known, at three different frequencies. Using the Coffey–Clem formula [195], they extracted the ρ_f as a fitting parameter, and found similar results as for UPt_3 and in YNi_2B_2C. Even in this case, however, because of the large crossover frequency, ω_p, free flux flow was not achieved without using any models. Recently, Umetsu *et al* [210] achieved free flux flow without using any models in LSCO, and succeeded in obtaining the magnetic field dependence of ρ_f from the experimental data alone. They found that, at high fields,

$$\rho_f \propto B^{\alpha} \tag{47}$$

with $\alpha < 1$, that is similar to the results obtained in other anisotropic SCs mentioned above. Therefore, it is likely that the strange magnetic field dependence of ρ_f is a common feature of anisotropic superconductors with gap nodes. This could be understood by the theory of Kopnin and Volovic [222], where ρ_f was given as

$$\rho_f = \frac{B}{ne\langle\omega_0\tau\rangle}, \tag{48}$$

where $\langle\,\rangle$ denotes the average over the Fermi surface. Because of the existence of the nodes in the order parameter, this could cause the enhanced ρ_f, also leading to the more gradual B dependence at higher B.

Recently, the existence of a collective mode in the microwave frequency range was predicted in unconventional superconductors with mixed symmetry order parameters [224]. Such a mode has not been observed in any experiments yet. This is another interesting problem.

In summary, flux flow of the vortex of HTSC has several new features, some of which might open a new category of physics, such as the energy dissipation of the quantum core. Theoretical investigation of the dynamics of such a quantum core is needed urgently.

6. Collective mode dynamics in cuprates

As was mentioned in the introductory section, microwave conductivity measurement was found to be very effective to explore the dynamics of collective modes in the quantum condensate. In particular, in strongly correlated materials, various kinds of interaction causes new ground states [5]. In this section, we will introduce two examples of microwave studies to look for the dynamics of the collective excitation characteristic of the strongly correlated systems in the cuprate superconductors and related materials.

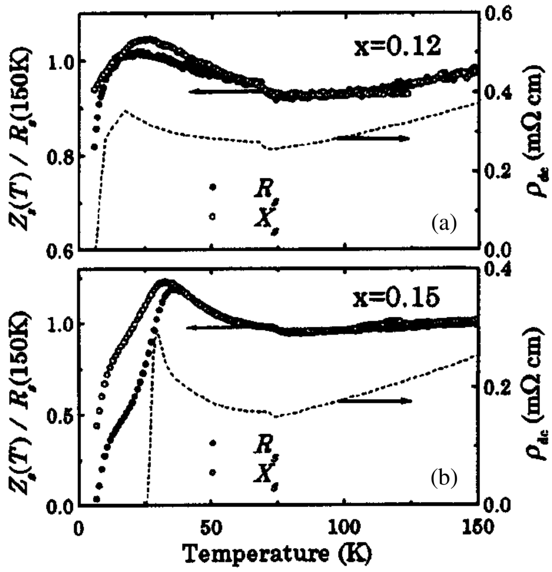

Figure 10. In-plane dc resistivity (dashed curve) and microwave surface impedance at 50 GHz of LNSCO as a function of temperature [226].

6.1. Can dynamics of charge stripes be seen?

The discovery of the static spin/charge stripe order in $La_{2-x-y}Nd_ySr_xCuO_4$ (LNSCO) by the elastic neutron scattering [225] has revealed that doped holes in the antiferromagnetic (AF) Mott insulators tend to segregate and form 'charge stripes', which are composite ordered structures of charge and spin. The Nd substitution induces a structural phase transition at a temperature T_{d2} ($\approx$80 K) from the low-temperature orthorhombic (LTO) to the low-temperature tetragonal (LTT) phase, which favours the static stripe ordering. Such periodic modulation of charge and spin configurations is quite reminiscent of the CDW or the SDW. Thus, it is expected that the dynamics of the stripe phase is considerably different from that of a Drude metal. In order to explore such a possibility, the temperature and frequency dependences of the in-plane conductivity of LNSCO ($x = 0.10$, 0.12, 0.15, $y = 0.4$) were investigated between microwave and optical regions [226, 227]. The microwave conductivity was measured at 10, 50 and 100 GHz. As is shown in figure 10, both R_s and X_s agree with each other at each temperature, showing the sample is in the Hagen–Rubens limit of the Drude conductivity. Thus, $\sigma_1 \simeq 1/\rho_1 \propto (1/R_s)^2 = (1/X_s)^2$. The temperature dependence of σ_{MW} was similar to that of $\sigma_{dc} \equiv 1/\rho_{dc}$, showing a small drop at T_{d2} ($\approx$70 K) and a weak semiconducting behaviour below T_{d2}, while the far-infrared conductivity, σ_{FIR}, above 40 cm^{-1} increased with decreasing temperature even below T_{d2}. There was no strong frequency dependence in σ_{MW} between 10 and 100 GHz ($\approx$0.3 and 3 cm^{-1}, respectively) even below T_{d2}. This observation ruled out the possibility of the extra contribution of the pinned collective mode in this frequency range. However, $\sigma(T)$ is very different between microwave and FIR regions, suggesting the existence of some structure in the conductivity spectrum in the intermediate frequency region. A recent optical study for LNSCO ($x = 0.125$, $y = 0.6$) showed that a finite-frequency peak in $\sigma_{FIR}(\omega)$ was developed between 15 and 100 cm^{-1} below T_{d2} [228]. The appearance of this peak can be attributed to the localization of charge carriers due to the reduction of the dimensionality caused by the formation of the static charge stripes.

In Nd-free $La_{2-x}Sr_xCuO_4$ (LSCO) and other orthorhombic cuprates, there was no structural phase transition to the LTT phase, and it is believed that the spin/charge stripe order fluctuates. It is also an interesting problem how the charge dynamics of fluctuating stripes show up in the ac conductivity in these materials. According to the neutron scattering study [229], the spin stripes (maybe also charge stripes) in LSCO with $x < 0.06$ are unidirectional and extend along the diagonal Cu–Cu direction of the CuO_2 planes ('diagonal stripes'), while the stripes in LSCO with $x > 0.06$ and LNSCO extend along the vertical (or horizontal) Cu–O–Cu direction ('vertical/horizontal stripes') and rotate away from each other by 90° between the neighbouring two CuO_2 layers. Dumm *et al* [230] have investigated the infrared conductivity of the lightly doped LSCO ($x = 0.03$, 0.04), and found that the Drude response seen above 80 K evolved into the finite-frequency peak centred at around 100 cm^{-1} below 80 K, which was similar to the peak observed in LNSCO. Recent complex conductivity measurements on LSCO films ($x = 0.04$–0.07) by the broadband techniques [48] also found that $\sigma_1(\omega)$ between 45 and 12 GHz above about 100 K could be regarded as that in the Hagen–Rubens limit of the Drude response, while $\sigma_1(\omega)$ for $x = 0.04$ increased slightly with increasing frequency below 100 K, implying a possible existence of the maximum in the conductivity spectrum at a much higher frequency region.

Thus, it is suggested that the charge dynamics in both the static and dynamical stripe phases is rather similar to that of the ordinary Drude metal, while the finite-frequency peak emerges in the conductivity spectrum in the localization regime at low temperatures, which seems to be a generic feature of low-dimensional disordered conductors.

6.2. A pinned collective mode in a two-leg ladder system

The hole-doped spin ladder system is a good reference to the high-T_c cuprates, since theories predicted the opening of the spin gap in even-leg spin ladders and the emergence of superconductivity by hole doping on such ladders [231]. Indeed, superconductivity appeared in $Sr_{14-x}Ca_xCu_{24}O_{41}$ (SCCO) along this scenario [232]. This material is a quasi-one-dimensional (Q1D) system, which contains planes of Cu_2O_3 two-leg ladders, planes of CuO_2 chains, and (Sr, Ca) layers. Since the average valence of Cu is +2.25 in the Ca-free material, holes are intrinsically doped in this compound. The isovalent substitution of Ca for Sr makes these self-doped holes redistribute from the CuO_2 chains to the Cu_2O_3 ladders, which effectively enables the hole doping on the two-leg ladders [233].

The charge dynamics along both the ladder (c-axis) and the rung (a-axis) directions of SCCO has been investigated in the microwave and millimetre wave regions between 30 and 100 GHz (figure 11) [234]. For the slightly hole-doped region ($x = 0$, 1, and 3), a small and narrow conductivity peak, centred around $\Omega_0/2\pi \sim 50$ GHz ($\sim$2.5 K), was observed in the frequency dependence of the c-axis conductivity $\sigma_1^c(T, \omega)$ below a temperature T^*, while there was no sign of a similar structure in the a-axis conductivity, $\sigma_1^a(T, \omega)$. Although T^* systematically decreased from 170 to 30 K with increasing x (from 0 to 3), the resonance-like conductivity peak ($\hbar\Omega_0 \sim 2.5$ K) can be observed up to moderately high temperatures ($\hbar\Omega_0 \ll k_B T^*$). Thus, the peak in σ_1^c cannot be attributed to any single-particle excitations. Instead, it should be attributed to some *collective* excitation, such as a pinned phason mode in the CDW and the SDW states. The existence of such a pinned collective mode was also suggested by succeeding experiments including the nonlinear dc conduction [234–237], the dielectric relaxation in the radio frequency region [235, 236, 238], and the electronic Raman scattering [236, 239].

Unfortunately, the origin of this collective mode has not been specified yet. However, the possibility of a charge-ordered state in the CuO_2 chain layers can be ruled out, because there

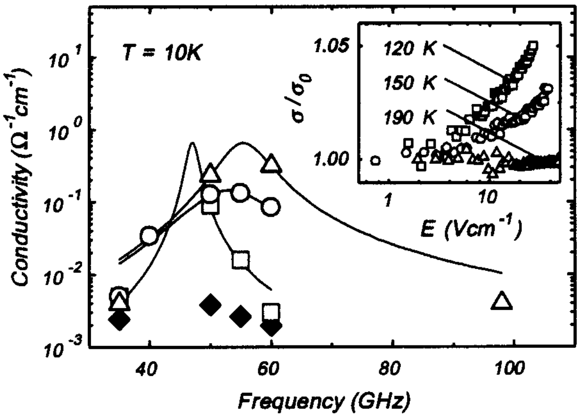

Figure 11. Microwave conductivity of a spin ladder, $Sr_{14}Cu_{24}O_{41}$ as a function of frequency. Different open marks correspond to σ_1^c in different samples, and the closed marks represent σ_1^a. The solid curve is a fit to a Lorentzian. The inset represents the dc nonlinear conductivity of the same material [234].

was no giant relaxation in the dielectric function of $La_3Sr_3Ca_8Cu_{24}O_{41}$, which had carriers only on the chain [240]. Therefore, the observed pinned collective mode should be associated with the charge-ordered state of doped holes on the *ladder* layers. Kitano *et al* estimated that the enhancement of the effective mass, m^*, was negligibly small, by relating the pinning frequency Ω_0 to the threshold field of the nonlinear dc conduction, E_0, in a single harmonic oscillator model [234]. Vuletić *et al* also concluded that the enhancement of m^* was only 20–50, by using an expression developed by Littlewood [241], which connects Ω_0 with the low-frequency dielectric relaxation time, τ_0 [238]. These results strongly suggest that the charge excitation in this material does not accompany lattice distortions, in contrast to the case of the conventional CDW materials. Thus, it is expected that a possible lattice distortion due to the charge-ordered state is too small to be observed by x-ray scattering.

To clarify the origin of the collective mode, it is also important to study the evolution of the collective excitations with Ca doping. The nonlinear dc conduction due to the sliding motion of the collective mode was found to disappear easily by the carrier doping [237]. On the other hand, the pinned collective mode in the microwave region was observed for $x = 0$–3. The giant dielectric relaxation in the radio-frequency region was also observed for $x = 0$–9 [238]. Interestingly, the temperature below which the giant dielectric relaxation was observed decreased with Ca doping systematically, similar to T^*. All these features may suggest that the charge-ordered state is unstable with the hole doping on ladders, while a finite spin gap remains to be opened even for $x > 10$ [242, 243].

However, at higher hole dopings ($x \geqslant 8$), there is still a debate. Osafune *et al* discovered a different conductivity peak at $\sim$100 cm^{-1} for $x = 8$, which was interpreted as another collective mode of hole pairs [244]. Recently, Vuletić *et al* proposed that it could be attributed to the opening of the CDW gap, based on the fact that the gap was suppressed systematically by the hole doping from $\sim$1000 cm^{-1} ($x = 0$) to $\sim$100 cm^{-1} ($x = 8$) [238]. On the other hand, a recent Raman scattering study reported that a fingerprint of the pinned collective mode was observed up to $\sim$600 K even for $x = 12$, implying that the quasiparticle gap was not suppressed by the hole doping [239]. To resolve the controversy, another interpretation was proposed, where this feature can be regarded as a generic feature of low-dimensional disordered conductors, similar to a finite-frequency peak in LNSCO and LSCO [228, 230].

To answer these questions clearly, detailed studies of conductivity in the microwave region are crucial even for these Ca-doped materials. Unfortunately, however, it becomes quite difficult to obtain $\sigma_{\rm MW}$ at higher hole dopings, since we require the analysis in the crossover region between SDR and DPR, as was discussed in section 3.2. We have investigated the microwave response at 35, 50, and 98 GHz for the $x = 12$ material, placed at the microwave electric field parallel to the c axis ($E_\omega \parallel c$). In contrast to the case of $x = 0$–3, the so-called depolarization peak, which is characteristic of the DPR, was no longer seen down to $\sim$5 K. We can make a rough estimate of the magnitude of the electric conductivity of unknown materials by the comparison of the microwave loss, $\Delta(1/2Q)$ at E_ω with that at the microwave magnetic field H_ω [245]. We found that $\Delta(1/2Q)$ at $H_\omega \perp ac$ plane was sufficiently larger than $\Delta(1/2Q)$ at $E_\omega \parallel c$. This suggests that the real part of $\sigma^c_{\rm MW}$ for $x = 12$ is much larger than that for $x = 0$–3, similar to the behaviour of $\sigma_{\rm dc}$. Although it is difficult to discuss the details of the frequency dependence of $\sigma_{\rm MW}$, a significant feature is that the collective excitation has not been observed between 30 and 100 GHz in the $x = 12$ material.

In summary, the collective charge excitation in these spin ladder materials is novel in the sense that this could be a new type of charge excitation that is characteristic of the strongly correlated low-dimensional systems. This surely deserves further studies. In addition to applying various new types of experiment, improvements in the microwave measurement techniques and the method of analysis are needed urgently.

7. Conclusion

In this article, recent studies of electromagnetic response at microwave- and millimetre-wave frequencies of the high-temperature cuprate superconductors and related materials were reviewed, with special interest in terms of the estimation of the complex conductivity in a wide range of materials with various conductivity magnitudes. Concerning the application of this technique to superconductors, thanks to the HTSC, our understanding of unconventional superconductivity achieved incredible progress in various aspects; each of them has been described above. At the same time, it also became clear that many issues have been remained unsettled, in spite of considerable efforts by many different groups. The above reviewed histories told us that all of the three important aspects of the research are inevitable: that is, the fabrication of samples (bulk single crystals or single-crystalline films) with very high quality, the development of new techniques with better resolution, sensitivity, and stability, and complete systematic study in a wide range of materials and doping. The microwave measurement techniques, when applied to other categories of materials, such as the ones undergoing the metal-to-insulator transition, are not well established. For this to be a more powerful tool, comprehensive approaches including a large-scale computer simulation, such as detailed analysis of electromagnetic field distribution for samples with arbitrary shape, etc might be necessary.

Acknowledgments

We thank T Hanaguri, D A Bonn, J Orenstein, Y Matsuda, Y Kato, and T Kita for fruitful discussions. This work was, in part, supported by a Grant-in-Aid for Scientific Research of the Ministry of Education, Science, Culture, and Sports in Japan.

References

[1] Wooten F 1972 *Optical Properties in Solids* (New York: Academic)
[2] Toyozawa Y 2003 *Optical Processes in Solids* (Cambridge: Cambridge University Press)
[3] Grüner G 1988 *Rev. Mod. Phys.* **60** 1129

[4] For example Ott H R 2002 *High-T_c Superconductivity* (*The Physics of Superconductors* vol 1) ed K H Bennemann and Ketterson (Berlin: Springer)
[5] Sachdev S 1999 *Quantum Phase Transitions* (Cambridge: Cambridge University Press)
[6] Pippard A B 1953 *Proc. R. Soc.* A **216** 547
[7] Biondi M A and Garfunkel M P 1957 *Phys. Rev.* **108** 495
[8] Pierce J M 1974 *Superconducting Microwave Resonators* (*Solid State Physics* vol 11) ed R V Coleman (New York: Academic) p 541
[9] Bonn D A and Hardy W N 1996 *Physical Properties of High Temperature Superconductors V* ed D M Ginsberg (Singapore: World Scientific)
[10] For a review Golosovsky M, Tsindlekht M and Davidov D 1996 *Supercond. Sci. Technol.* **9** 1
[11] Kuriki S *et al* 2003 *Vortex Electronics and SQUIDs* ed T Kobayashi, H Hayakawa and M Tonouchi (Berlin: Springer)
[12] London H 1934 *Nature* **133** 497
[13] Bardeen J, Cooper L N and Schrieffer J R 1957 *Phys. Rev.* B **106** 162
Bardeen J, Cooper L N and Schrieffer J R 1957 *Phys. Rev.* B **108** 1175
[14] Bardeen J and Schrieffer J R 1961 *Progress on Low Tempearture Physics* vol 3, *Recent Developments in Superconductivity* ed C J Gorter (Amsterdam: North-Holland) p 1
[15] Tinkham M 1996 *Introduction to Superconductivity* 2nd edn (New York: McGraw-hill)
[16] Panagopoulos C *et al* 1997 *Phys. Rev. Lett.* **79** 2320 and references cited therein
[17] Panagopoulos C *et al* 1998 *Phys. Rev. Lett.* **81** 2336 and references cited therein
[18] Porch A *et al* 1993 *Physica* C **214** 350
[19] Klein O *et al* 1993 *Int. J. Infrared Millim. Waves* **14** 2423
[20] Donovan S *et al* 1993 *Int. J. Infrared Millim. Waves* **14** 2459
[21] Dressel M *et al* 1993 *Int. J. Infrared Millim. Waves* **14** 2489
[22] Sridhar S and Kennedy W L 1988 *Rev. Sci. Instrum.* **59** 531
[23] Rubin D L *et al* 1988 *Phys. Rev.* B **38** 6538
[24] Hardy W N and Whitehead L A 1981 *Rev. Sci. Instrum.* **52** 213
[25] Bonn D A, Morgan D C and Hardy W N 1991 *Rev. Sci. Instrum.* **62** 1819
[26] Hardy W N *et al* 1993 *Phys. Rev. Lett.* **70** 3999
[27] Schawlow A L and Dvlin G E 1939 *Phys. Rev.* **113** 120
[28] Clover R B and Wolf W P 1970 *Rev. Sci. Instrum.* **41** 617
[29] Slavin A J 1972 *Cryogenics* **12** 121
[30] Maeda A *et al* 1992 *Phys. Rev.* B **46** 14234
[31] Carrington A *et al* 1999 *Phys. Rev.* B **59** R14173
[32] Hanaguri T *et al* 2003 *Rev. Sci. Instrum.* **74** 4436
[33] Kokales J D *et al* 2000 *Physica* C **341–348** 1655
[34] Taber R C 1990 *Rev. Sci. Instrum.* **61** 2200
[35] Langley B W *et al* 1991 *Rev. Sci. Instrum.* **62** 1801
[36] Klein N *et al* 1992 *J. Supercond.* **5** 195
[37] Turneaure S J *et al* 1998 *J. Appl. Phys.* **83** 4334
[38] Petersan P J and Anlage S M 1998 *J. Appl. Phys.* **84** 3392
[39] Inoue R *et al* 2004 *IEEE Trans. Microw. Theory Tech.* **52** 2163
[40] Matsuda Y *et al* 1994 *Phys. Rev.* B **49** 4380
[41] Turner P J *et al* 2003 *Phys. Rev. Lett.* **90** 237005
[42] Turner P J *et al* 2004 *Rev. Sci. Instrum.* **75** 124
[43] Gaifullin M B *et al* 1999 *Phys. Rev. Lett.* **83** 3928
[44] Gaifullin M B *et al* 2000 *Phys. Rev. Lett.* **84** 2945
[45] Booth J C *et al* 1994 *Rev. Sci. Instrum.* **65** 2082
[46] Booth J C *et al* 1996 *Phys. Rev. Lett.* **77** 4438
[47] Tosoratti A *et al* 2000 *Int. J. Mod. Phys.* B **14** 2926
[48] Kitano H *et al* 2004 *Physica* C **412–414** 130
[49] Stutzman M L, Lee M and Bradley R F 2000 *Rev. Sci. Instrum.* **71** 4596
[50] Bonn D A *et al* 1994 *Phys. Rev.* B **50** 4051
[51] Tsuchiya Y, Iwaya K, Kinoshita K, Hanaguri T, Kitano H, Maeda A, Shibata K, Nishizaki T and Kobayashi N 2001 *Phys. Rev.* B **63** 184517
[52] Hosseini A *et al* 1999 *Phys. Rev.* B **60** 1349
[53] Lee S F *et al* 1996 *Phys. Rev. Lett.* **77** 735
[54] Buravov L I and Shchegolev I F 1971 *Instrum. Exp. Tech.* **14** 528

[55] Inoue R, Kitano H and Maeda A 2005 *Microelectron. J.* submitted
[56] Champlin K S and Krongard R R 1961 *IRE Trans. Microw. Theory Tech.* **9** 545
[57] Tompkin J and Spencer E G 1957 *J. Appl. Phys.* **28** 969
[58] Brodwin B E and Parsons M K 1965 *J. Appl. Phys.* **36** 494
[59] Inoue R, Kitano H and Maeda A 2003 *J. Appl. Phys.* **93** 2736
[60] Inoue R, Kitano H and Maeda A 2003 *Physica* B **329–333** 1546
[61] Ong N P 1977 *J. Appl. Phys.* **48** 2435
[62] Kitano H 1999 *Thesis* University of Tokyo
[63] Annet J 1990 *Adv. Phys.* **39** 83
[64] Mattis D C and Bardeen J 1958 *Phys. Rev.* **111** 412
[65] Hirschfeld P J *et al* 1993 *Phys. Rev.* B **50** 10230
[66] Hebel L C and Slichter C P 1959 *Phys. Rev.* **113** 1504
[67] Holczer K, Klein O and Gruener G 1991 *Solid State Commun.* **78** 875
[68] Abrikosov A A, Gorkov L P and Khalatonikov L P 1959 *J. Exp. Theor. Phys.* **35** 1
[69] Ryckayzen G 1965 *Theory of Superconductivity* (New York: Interscience)
[70] For a review of early results, see for example Madea A, Tajima S and Kitazawa K 1993 *Mater. Sci. Forum* **137–139** 1
[71] Anlage S M *et al* 1991 *Phys. Rev.* B **44** 9764
[72] Cooper J R *et al* 1990 *Solid State Commun.* **75** 737
[73] Ma Z G *et al* 1993 *Phys. Rev. Lett.* **71** 781
[74] Erb A, Walker E and Flükiger R 1995 *Physica* C **245** 245
[75] Srikanth H *et al* 1997 *Phys. Rev.* B **55** R14733
[76] Kamal S *et al* 1998 *Phys. Rev.* B **58** R8933
[77] Liang R *et al* 1998 *Physica* C **304** 105
[78] Anlage S M *et al* 1994 *Phys. Rev.* B **50** 523
[79] Shibauchi T *et al* 1996 *Physica* C **264** 227
[80] Jacobs T *et al* 1995 *Phys. Rev. Lett.* **75** 4516
[81] Hanaguri T *et al* 1999 *Phys. Rev. Lett.* **82** 1273
[82] Broun D M *et al* 1997 *Phys. Rev.* B **56** R11443
[83] Scalapino D J 1995 *Phys. Rep.* **250** 329
[84] Dessau D S *et al* 1991 *Phys. Rev. Lett.* **66** 2160
[85] Harlingen D J 1995 *Rev. Mod. Phys.* **67** 515
[86] Shibauchi T *et al* 1994 *Phys. Rev. Lett.* **72** 2263
[87] Paget K M *et al* 1999 *Phys. Rev.* B **59** 641
[88] Hirschfeld P J and Goldenfeld N 1993 *Phys. Rev.* B **48** 4219
[89] Pan S H *et al* 2000 *Phys. Rev. Lett.* **85** 1536
[90] Balatsky A V, Kumar P and Schrieffer J R 2000 *Phys. Rev. Lett.* **84** 4445
[91] Bonn D A *et al* 1996 *Czech. J. Phys.* **46** (Suppl. S6) 3195
[92] Uemura Y J *et al* 1989 *Phys. Rev. Lett.* **62** 2317
[93] Lee P A and Wen X-G 1997 *Phys. Rev. Lett.* **78** 4111
[94] Hosseini A *et al* 2004 *Phys. Rev. Lett.* **93** 107003
[95] Sheehy D E, Davis T P and Franz M 2004 *Phys. Rev.* B **70** 054510
[96] Matsukawa H and Fukuyama H 1989 *J. Phys. Soc. Japan* **58** 2845
Matsukawa H and Fukuyama H 1989 *J. Phys. Soc. Japan* **58** 3687
[97] Kashiwaya S *et al* 1998 *Phys. Rev.* B **57** 8680
[98] Alff L *et al* 1998 *Phys. Rev.* B **58** 11197
[99] Chen C T *et al* 2002 *Phys. Rev. Lett.* **88** 227002
[100] Tsui C C and Kirtley J R 2000 *Phys. Rev. Lett.* **85** 182
[101] Armitage N P *et al* 2001 *Phys. Rev. Lett.* **86** 1126
[102] Wu D H *et al* 1993 *Phys. Rev. Lett.* **70** 85
[103] Cooper J R *et al* 1996 *Phys. Rev.* B **54** R3753
[104] Naito M and Sato H 1995 *Appl. Phys. Lett.* **67** 2557
[105] Alff L *et al* 1999 *Phys. Rev. Lett.* **83** 2644
[106] Prozorov R *et al* 2000 *Phys. Rev. Lett.* **85** 3700
[107] Kokales J D *et al* 2000 *Phys. Rev. Lett.* **85** 3696
[108] Skinta J A *et al* 2002 *Phys. Rev. Lett.* **88** 207005
[109] Biswas A *et al* 2002 *Phys. Rev. Lett.* **88** 207004
[110] Kim M S *et al* 2003 *Phys. Rev. Lett.* **91** 087001

[111] Snezhko A *et al* 2004 *Phys. Rev. Lett.* **92** 157005
[112] Maeda A 1998 *Supercond. Rev.* **3** 1
[113] Yip S K and Suals J 1992 *Phys. Rev. Lett.* **69** 2264
[114] Maeda A 1995 *Phys. Rev. Lett.* **74** 1202
[115] Maeda A 1996 *J. Phys. Soc. Japan* **65** 3638
[116] Bidinosti C P *et al* 2001 *Phys. Rev. Lett.* **86** 1074
[117] Maeda A *et al* 1999 *J. Phys. Soc. Japan* **68** 594
[118] Jujo T 2002 *Thesis* Kyoto University
[119] Shibauchi T *et al* 1992 *Physica* C **315–319** 127
[120] Halbritter J 1992 *J. Appl. Phys.* **71** 339
[121] Lee P A 1993 *Phys. Rev. Lett.* **71** 1887
[122] Imai T *et al* 1988 *J. Phys. Soc. Japan* **57** 2280
[123] Nuss M C *et al* 1991 *Phys. Rev. Lett.* **66** 3305
[124] Bonn D A *et al* 1992 *Phys. Rev. Lett.* **68** 2390
[125] Bonn D A *et al* 1993 *Phys. Rev.* B **47** 11314
[126] Krishana K *et al* 1999 *Phys. Rev. Lett.* **82** 5108
[127] Hettler M H and Hirshfeld P J 2000 *Phys. Rev.* B **61** 11313
[128] Harris R *et al* 2001 *Phys. Rev.* B **64** 064509
[129] Shibauchi T *et al* 1996 *J. Phys. Soc. Japan* **65** 3266
[130] Mochiku T and Kadowaki K 1993 *Trans. Mater. Res. Soc. Japan* **19A** 349
[131] Corson J *et al* 2000 *Phys. Rev. Lett.* **85** 2569
[132] Valla T *et al* 1999 *Science* **285** 2110
[133] Kaminski A *et al* 2000 *Phys. Rev. Lett.* **84** 1788
[134] Ando Y *et al* 2000 *Phys. Rev.* B **62** 626
[135] Ioffe L B and Millis A J 1998 *Phys. Rev.* B **58** 11631
[136] Norman M R *et al* 1998 *Nature* **392** 157
[137] Lang K M *et al* 2002 *Nature* **415** 412
[138] Gedik N *et al* 2003 *Science* **300** 1410
Gedik N *et al* 2003 *Preprint* condmat-0309121
[139] For a review Cooper S L and Gray K E 1994 *Physical Properties of High Temperature Superconductors IV* ed D M Ginsberg (Singapore: World Scientific) p 61
[140] Anderson P W 1992 *Science* **256** 1526
[141] Lawrence W and Doniach S 1971 *Proc. 12th Int. Conf. on Low Temperature Physics* ed E Kanda (Kyoto: Academic) p 361
[142] Ambegaokar V and Baratoff A 1963 *Phys. Rev. Lett.* **10** 486
Ambegaokar V and Baratoff A 1963 *Phys. Rev. Lett.* **11** 104 (erratum)
[143] Hosseini A, Kamal S, Bonn D A, Liang R and Hardy W N 1998 *Phys. Rev. Lett.* **81** 1298
[144] Kitano H *et al* 2001 *Physica* C **362** 247
[145] Radtke R J, Kostur V N and Levin K 1996 *Phys. Rev.* B **53** R522
[146] Graf M *et al* 1994 *Physica* C **235–240** 3271
[147] Hirschfelt P J, Quinlan S M and Scalapino D J 1997 *Phys. Rev.* B **55** 12742
[148] Anderson O K *et al* 1996 *Phys. Rev.* B **49** 4145
[149] van der Marel D 1999 *Phys. Rev.* B **60** R765
[150] Xiang T and Wheatley J M 1996 *Phys. Rev. Lett.* **77** 4632
[151] Wheatley J M, Hsu T C and Anderson P W 1988 *Phys. Rev.* B **37** 5897
[152] Chakravarty S *et al* 1993 *Science* **261** 337
[153] Xiang T and Wheatley J M 1996 *Phys. Rev. Lett.* **76** 134
[154] Tsvetkov A A *et al* 1998 *Nature* **395** 360
[155] Liang R *et al* 2002 *Physica* C **383** 1
[156] Gough C E and Exon N J 1994 *Phys. Rev.* B **50** 488
[157] Ioffe L B and Millis A J 2002 *J. Phys. Chem. Solids* **63** 2259
[158] Kitano H *et al* 1995 *Phys. Rev.* B **51** 1401
[159] Mao J *et al* 1995 *Phys. Rev.* B **51** 3316
[160] Nefyodov Y A *et al* 2003 *Phys. Rev.* B **67** 144504
[161] Schützmann J *et al* 1995 *Phys. Rev.* B **52** 13665
[162] Homes C C *et al* 1995 *Physica* C **254** 265
[163] Xiang T and Hardy W N 2000 *Phys. Rev.* B **63** 024506
[164] Kitano H *et al* 1998 *Phys. Rev.* B **57** 10946

[165] Kitano H *et al* 1999 *J. Low Temp. Phys.* **117** 1241
[166] Shafranjuk S E *et al* 1997 *Phys. Rev.* B **55** 8425
[167] Artemenko S N *et al* 1999 *Phys. Rev.* B **59** 11587
[168] Dulić D *et al* 1999 *Phys. Rev.* B **60** R15051
[169] Latyshev Y I *et al* 1999 *Phys. Rev. Lett.* **82** 5345
[170] For example Scott W C 1970 *Appl. Phys. Lett.* **17** 166
[171] For a review of early theoretical and experimental works, see Skocpol W J and Tinkham M 1975 *Rep. Prog. Phys.* **38** 1049 and references therein
[172] Aslamazov L G and Larkin A I 1968 *Phys. Lett.* A **26** 238
[173] Maki K 1968 *Prog. Theor. Phys.* **40** 193
Thompson R S 1970 *Phys. Rev.* B **1** 327
[174] Schmidt H 1968 *Z. Phys.* **215** 210
Schmidt H 1970 *Z. Phys.* **232** 443
[175] Lehoczky S L and Briscoe C V 1971 *Phys. Rev.* B **4** 3938
[176] Fisher D S, Fisher M P A and Huse D A 1991 *Phys. Rev.* B **43** 130
[177] Kamal S *et al* 1994 *Phys. Rev. Lett.* **73** 1845
[178] Horbach M L and van Saarloos W 1992 *Phys. Rev.* B **46** 432
[179] Olsson H K and Koch R H 1992 *Phys. Rev. Lett.* **68** 2406
[180] Anlage S *et al* 1996 *Phys. Rev.* B **53** 2792
[181] Waldram J R *et al* 1999 *Phys. Rev.* B **59** 1528
[182] Peligrad D-N, Mehring M and Dulčić A 2003 *Phys. Rev.* B **67** 174515
[183] Dorsey A T 1991 *Phys. Rev.* B **43** 7575
[184] Hohenberg P C and Halperin B I 1977 *Rev. Mod. Phys.* **49** 435
[185] Kosterlitz J M and Thouless D J 1973 *J. Phys. C: Solid State Phys.* **6** 1181
[186] Wickham R A and Dorsey A T 2000 *Phys. Rev.* B **61** 6945
[187] Corson J *et al* 1999 *Nature* **398** 221
[188] Buzdin A I and Feinberg D 1990 *J. Physique* **51** 1971
Artemenko S N and Kruglov A N 1990 *Phys. Lett.* A **143** 485
Clem J R 1991 *Phys. Rev.* B **43** 7837
[189] Clem J R and Coffey M W 1990 *Phys. Rev.* B **42** 6209
[190] Tachiki M and Takahashi S 1989 *Solid State Commun.* **72** 1083
[191] Bardeen J and Stephen M J 1965 *Phys. Rev.* **140** A1197
[192] Kita T 2003 *Preprint* cond-mat/0307067
[193] Gittleman J I and Rosenblum B 1966 *Phys. Rev. Lett.* **16** 734
[194] Anderson P W 1962 *Phys. Rev. Lett.* **9** 309
Anderson P W and Kim Y B 1964 *Rev. Mod. Phys.* **36** 39
[195] Coffey M W and Clem J R 1991 *Phys. Rev. Lett.* **67** 386
[196] Caroli C, de Gennes P G and Matricon J 1964 *Phys. Lett.* **9** 307
[197] Hess H F, Robinson R B, Dynes R C, Valles J M and Waszczak J V 1989 *Phys. Rev. Lett.* **62** 214
[198] Blatter G *et al* 1994 *Rev. Mod. Phys.* **66** 1125
[199] Kopnin N B and Kravtsov V E 1976 *Pis. Zh. Eksp. Teor. Fiz.* **23** 631
Kopnin N B and Kravtsov V E 1976 *Sov. Phys.—JETP Lett.* **23** 578 (Engl. Transl.)
[200] Volovik G E 1993 *Pis. Zh. Eksp. Teor. Fiz.* **58** 457
Volovik G E 1993 *JETP Lett.* **58** 469 (Engl. Transl.)
Schopohl N and Maki K 1995 *Phys. Rev.* B **52** 490
Ichioka M, Hayashi Y, Enomoto N and Machida K 1996 *Phys. Rev.* B **53** 15316
[201] Wang Y and MacDonald A H 1995 *Phys. Rev.* B **52** R3876
[202] Maggio-Aprile I, Renner Ch, Erb A, Walker E and Fischer O 1995 *Phys. Rev. Lett.* **75** 2754
[203] Renner Ch, Ravaz B, Kadowaki K, Maggio-Aprile I and Fischer O 1998 *Phys. Rev. Lett.* **80** 3606
[204] Kopnin N and Volovik G E 1997 *Phys. Rev. Lett.* **79** 1377
[205] Pambianchi M S, Wu D H, Ganapathi L and Anlage S M 1993 *IEEE Trans. Appl. Supercond.* **3** 2774
[206] Morgan D C, Zhang K, Bonn D A, Liang R, Hardy W N, Kallin C and Berlinsky A J 1994 *Physica* C **235–240** 2015
[207] Revenaz S, Oates D E, Labb'e-Lavigne D, Dresselhaus G and Dresselhaus M S 1994 *Phys. Rev.* B **50** 1178
[208] Parks B, Spielman S, Orenstein J, Nemeth D T, Ludwig F, Clarke J, Marchant P and Lew D J 1995 *Phys. Rev. Lett.* **74** 3265
[209] Maeda A *et al* 2001 *Physica* C **362** 127
[210] Umetsu T *et al* 2002 unpublished

[211] Kuncuer M *et al* 2001 *Phys. Rev. Lett.* **87** 177001
Kuncuer M *et al* 2002 *Phys. Rev. Lett.* **89** 137005
[212] Kinoshita K *et al* 2003 *Physica* C **388–389** 417
Kinoshita K *et al* 2004 *Physica* C **412–414** 530
[213] Tsuchiura H 2003 *Phys. Rev.* B **52** 012509
[214] Himeda A, Ogata M, Tanaka Y and Kashiwaya S 1997 *J. Phys. Soc. Japan* **66** 3367
Ogata M 1999 *Int. J. Mod. Phys.* B **13** 3560
Han J H and Lee D H 2000 *Phys. Lett.* **85** 1100
[215] Lake B *et al* 2001 *Science* **291** 1759
[216] Kakuyanagi K, Kumagai K and Matsuda Y 2002 *Phys. Rev.* B **65** 060503
Kakuyanagi *et al* 2003 *Phys. Rev. Lett.* **90** 197003
[217] Mitrovic V F *et al* 2001 *Nature* **413** 501
[218] Hoffman J H, Hudson E W, Lang K M, Madhaven V, Eisaki H, Uchida S and Davis J C 2002 *Science* **295** 466
[219] Kambe S *et al* 1999 *Phys. Rev. Lett.* **83** 1842
[220] Takaki K *et al* 2002 *Phys. Rev.* B **66** 184511
[221] Matsuda Y 2002 *Phys. Rev.* B **66** 945
Izawa K *et al* 2000 *Physica* B **284–288** 945
[222] Kopnin N B 2001 *Theory of Nonequilibrium Superconductivity* (Oxford: Oxford University Press) and references cited therein
[223] Hanaguri T, Tsuboi T, Tsuchiya Y, Sasaki K and Maeda A 1999 *Phys. Rev. Lett.* **82** 1273
[224] Balatsky A V, Kumar P and Schrieffer J R 2000 *Phys. Rev. Lett.* **84** 4445
[225] Tranquada J *et al* 1995 *Nature* **375** 561
[226] Tajima S *et al* 1999 *Europhys. Lett.* **47** 715
[227] Tajima S *et al* 2000 *Physica* C **341–348** 1723
[228] Dumm M *et al* 2002 *Phys. Rev. Lett.* **88** 147003
[229] Matsuda M *et al* 2000 *Phys. Rev.* B **62** 9148
[230] Dumm M *et al* 2003 *Phys. Rev. Lett.* **91** 077004
[231] For a review, see Dagotto E 1999 *Rep. Prog. Phys.* **62** 1525
[232] Uehara M *et al* 1996 *J. Phys. Soc. Japan* **65** 2764
[233] Osafune T *et al* 1997 *Phys. Rev. Lett.* **78** 1980
[234] Kitano H *et al* 2001 *Europhys. Lett.* **56** 434
[235] Gorshunov B *et al* 2002 *Phys. Rev.* B **66** 060508(R)
[236] Blumberg G *et al* 2002 *Science* **297** 584
[237] Maeda A *et al* 2003 *Phys. Rev.* B **67** 115115
[238] Vuletić T *et al* 2003 *Phys. Rev. Lett.* **90** 257002
[239] Gozar A *et al* 2003 *Phys. Rev. Lett.* **91** 087401
[240] Vuletić T *et al* 2003 *Phys. Rev.* B **67** 184521
[241] Littlewood P B 1987 *Phys. Rev.* B **36** 3108
[242] Kumagai K *et al* 1997 *Phys. Rev. Lett.* **78** 1992
[243] Katano S *et al* 1999 *Phys. Rev. Lett.* **82** 636
[244] Osafune T *et al* 1999 *Phys. Rev. Lett.* **82** 1313
[245] Kitano H *et al* 2002 *Phys. Rev. Lett.* **88** 096401